

OCT 8 1952

c.2

NACA TN 2790

# NATIONAL ADVISORY COMMITTEE FOR AERONAUTICS

TECHNICAL NOTE 2790

FLOW STUDIES IN THE VICINITY OF A MODIFIED FLAT-PLATE  
RECTANGULAR WING OF ASPECT RATIO 0.25

By William H. Michael, Jr.

Langley Aeronautical Laboratory  
Langley Field, Va.



Washington  
September 1952

NACA LIBRARY  
LANGLEY AERONAUTICAL LABORATORY  
Langley Field, Va.

## NATIONAL ADVISORY COMMITTEE FOR AERONAUTICS

## TECHNICAL NOTE 2790

## FLOW STUDIES IN THE VICINITY OF A MODIFIED FLAT-PLATE

## RECTANGULAR WING OF ASPECT RATIO 0.25

By William H. Michael, Jr.

## SUMMARY

An investigation was made in order to study the characteristics of the flow in the vicinity of a rectangular wing of aspect ratio 0.25 with a modified flat-plate airfoil section. The investigation was conducted by means of photographs of a tuft grid located at a number of chordwise positions along the airfoil and behind the trailing edge of the airfoil. Supplementary measurements of the vorticity distribution in the wake were made with a yaw-head pitot-tube installation.

The results indicate that there is a rapid rolling-up of the trailing vorticity along the chord of the wing and that at the higher angles of attack there is a distinct vortex visible at the first chordwise station behind the leading edge considered (12.5 percent chord). The trailing vortex sheet is apparently immediately rolled up into the vortex cores. The vertical locations of the vortex cores appear to leave the wing at approximately the 12.5-percent-chord position with an initial slope somewhat less than the angle of attack of the wing. The slope is approximately equal to one-half the angle of attack at the trailing edge and decreases somewhat behind the trailing edge. The slopes of the vertical locations of the vortex cores are predicted very well by the theory of Bollay.

The photographs used in the present study show no clearly defined lateral movement of the cores with increasing angle of attack. The chordwise growth of lift calculated from the trailing-vortex strengths shows that the lift increases fairly rapidly across the forward part of the chord with approximately 70 to 85 percent of the total wing lift present forward of the midchord position. The total lift calculated from the tuft-grid photographs showed good agreement with the lift measured on the balance system.

## INTRODUCTION

Lifting surfaces of small aspect ratio have been used as vertical tail surfaces on conventional aircraft for some time and recently have come into increased prominence for general use in missile designs and as wings on high-speed aircraft. In order to meet the need for information regarding the aerodynamic characteristics of wings of small aspect ratio, a number of theoretical approaches have been developed and some experimental work has been done. A summary of available theories and tests of wings of small aspect ratio is given in reference 1. Some of the theories constitute extensions of lifting-line and lifting-surface theories to wings of small aspect ratio and some approximate the nonlinear features of the problem. Most of the theories contain simplifying assumptions concerning the trailing-vortex sheet. In view of the current interest in low-aspect-ratio lifting surfaces and the nonlinear nature of the behavior arising from the increased importance of viscous effects on low-aspect-ratio lifting surfaces where the viscous run is large, the physical characteristics of the flow in the vicinity of such low-aspect-ratio surfaces should be ascertained, not only as a matter of general interest, but also in order to establish a basis for additional theoretical considerations.

The present paper presents the results of flow studies of a rectangular wing of aspect-ratio 0.25 with a modified flat-plate airfoil section. The studies have been made by means of photographs of a tuft grid located at a number of chordwise positions along the airfoil and in the wake of the airfoil. Additional wake surveys with a yaw-head pitot-tube installation supplement the tuft-grid results. The results are believed to give a good qualitative indication of the flow phenomena associated with airfoils of low aspect ratio.

## SYMBOLS

The positive directions of forces, moments, and angles used in presenting the force data of this paper are shown in figure 1. The symbols used herein are defined as follows:

A	aspect ratio
$\alpha$	wing angle of attack, deg
c	wing chord, ft
ds	incremental distance, ft (see fig. 8).

$q$	dynamic pressure, lb/sq ft
$V_t$	tangential velocity, ft/sec
$V$	free-stream velocity, ft/sec
$S$	wing area, sq ft
$\Gamma$	circulation, sq ft per sec
$\gamma$	vorticity, $\frac{\Gamma}{\text{Area}}$ , per sec
$L$	lift, lb
$M$	pitching moment, ft-lb, measured about quarter-chord position
$D$	drag, lb
$C_L$	lift coefficient, $L/qS$
$(C_L)_{\text{chord}}$	lift coefficient at a particular chord position
$C_m$	pitching-moment coefficient, $M/qSc$
$C_D$	drag coefficient, $D/qS$

#### APPARATUS AND TESTS

The model used in this investigation consisted of a modified flat-plate rectangular mahogany wing with a thickness ratio of approximately 2 percent. The leading edge and tips were rounded, and the afterpart was beveled from the 75-percent-chord position to the trailing edge. A line drawing of the model is given in figure 2(a).

A tuft grid was used to study the flow in the vicinity of the wing. The grid consisted of a tubular frame with intersecting pieces of fine wire (0.012-inch diameter) spaced at 1-inch horizontal and vertical distances. At each intersection was attached a wool tuft 3 inches in length. (See fig. 2(b).) Viewed from a position far downstream, the horizontal and vertical components of the tuft projections are proportional to the angles of sidewash and downwash at the tuft locations (ref. 2).

Parts of the horizontal and vertical wires were omitted in the center of the grid to allow the grid to be placed at various chordwise positions along the wing. In order to test the chordwise positions between the leading and trailing edges of the wing, the grid was mounted at a constant position immediately behind the thin streamlined support strut and the model was mounted on the support strut at the specified chordwise positions (see fig. 2). In order to test the chordwise positions in front of the leading edge or behind the trailing edge, the model was mounted at the midchord position and the grid was placed in front of or behind the wing. Tests were made with the grid located at the following relative chordwise positions: at the leading edge; 12.5, 25, 37.5, 50, 62.5, and 75 percent chord behind the leading edge; at the trailing edge; and 25 and 50 percent chord behind the trailing edge. The chord of the wing was 48 inches.

The tests consisted of angle-of-attack runs at a dynamic pressure of 8 pounds per square foot (corresponding to a Reynolds number of  $2.09 \times 10^6$  based on the wing chord) for each of the 10 grid positions. An aerial camera located far downstream was used to photograph the grid at each  $2^\circ$  increment of wing angle of attack through an angle-of-attack range from  $0^\circ$  to  $30^\circ$ . Force measurements were made on the balance system for the angle-of-attack range.

Additional studies of the vorticity distribution in the wake were made with a yaw-head pitot-tube installation. By means of a gearing arrangement, the yaw-head pitot tube was rotated through a complete circle of 1.67-inch radius in a plane perpendicular to the free-stream velocity. The tangential velocity on the circumference of the circle could be determined from the velocity and angular readings of the yaw-head pitot tube and thus the average circulation over a small area could be determined. This arrangement was used to find the vorticity distribution in a plane approximately 3.5 inches (7 percent chord) behind the trailing edge of the wing at a wing angle of attack of  $20^\circ$  and a Reynolds number of  $2.09 \times 10^6$ .

Jet-boundary corrections were made for the lift and drag coefficients and angle of attack in the force-test data, but none were made in the tuft-grid-photograph results because the corrections (less than  $2^\circ$  at the maximum lift coefficient) were considered to be of the same order as the probable errors involved in estimating the tuft projections and vortex-core positions.

## RESULTS AND DISCUSSION

## Force-Test Results

The longitudinal aerodynamic characteristics of the model are presented in figure 3, and a comparison of the measured lift curve with other measured and theoretical results from references 3 to 5 is presented in figure 4. For the lift-curve comparisons, the results of the references were interpolated to obtain the results for  $A = 0.25$ .

One basic characteristic of low-aspect-ratio wings, the nonlinear variation of the lift with angle of attack, is illustrated in the comparison of the lift measured in the present tests with the linear-theory calculations of reference 6. (See fig. 4.) Large changes in the chordwise loading are characteristic of the deviation from linear theory as is illustrated by the center-of-pressure positions shown in figure 3(b). The center-of-pressure positions, which are shown to be variable with the wing angle of attack, move rearward as the angle of attack is increased. This rearward movement of the center of pressure might be explained in a simple manner by using the concept of viscous loading presented in reference 7. The viscous loading, which is caused by separation at the edges of the wing and which is assumed to be constant across the chord with its center of pressure at the midchord position, increases more rapidly with  $\alpha$  (proportional to  $\alpha^2$ ) than does the perfect fluid loading of reference 6. This condition causes the actual center of pressure to move rearward with increase in  $\alpha$ . It is interesting to note that the drag coefficient is very nearly equal to the product of the lift coefficient and the tangent of the angle of attack plus the drag at zero angle of attack. This fact indicates that the resultant force vector is approximately normal to the wing at the higher angles of attack.

## Formation of Vortices and Vorticity Distribution in the Wake

The tuft-grid test results, upon which most of the present analysis is based, are presented in the photographs of figure 5. Each part of figure 5 contains the complete set of chordwise grid positions for a particular angle of attack. In the photographs of the grid located at the trailing edge and positions behind the trailing edge, a line representing the extension of the chord plane has been inserted.

From the photographs, it appears that a characteristic of very-low-aspect-ratio wings is the rapid rolling-up of the trailing vorticity, not only behind the trailing edge, but also along the chord of the wing. At the higher angles of attack, a distinct vortex is plainly visible at

the first chordwise station behind the leading edge considered; that is, at the 12.5-percent-chord position. Reference 8 points out that for low-aspect-ratio wings it is possible for the vortex sheet to become completely rolled up within one chord length or less behind the trailing edge. This is apparently the case for the model of the present investigation. The vortices formed along the wing chord increased in strength toward the trailing edge, and immediately behind the trailing edge there was no visible evidence of a vortex sheet.

As a supplementary investigation of the wake characteristics, the yaw-head pitot tube was used to find the average vorticity for a number of small circles with radii of 1.67 inches in a plane approximately 3.5 inches (7 percent chord) behind the trailing edge of the wing at  $\alpha = 20^\circ$ . Yaw-head pitot-tube readings were taken at  $60^\circ$  intervals on the circumference of the circles. The value of the vorticity calculated for each circle was assumed to be the average vorticity for a small area with its center at the center of the circle and was plotted at a point representing the center of the circle. Contours of constant values of

average vorticity  $\gamma = \frac{\Gamma}{\text{Area of circle}}$  are presented in figure 6. It should be pointed out here that the finite size of the circles used in obtaining the average vorticity for figure 6 causes a severe reduction in the peaks of the vorticity distribution. Actually, the values of the average vorticity near the vortex core might be found to be considerably higher if a smaller size circle were used. The figure is included to indicate the location of the vortex core rather than to indicate the exact extent and magnitude of the vorticity distribution.

Figure 6 shows that most of the vorticity is concentrated in the area in which the photographs indicate a trailing vortex is to be found but that the vortex sheet, which extends downward from the vortex core, contains a small amount of vorticity which is not yet rolled up. Such a distribution of vorticity along the vortex sheet has also been observed qualitatively for this and other wings by use of a small tuft attached to a probe which is moved about in the wing wake. A twirling of the tuft indicates a region containing vorticity. The existence of such a region indicates that some of the vorticity in the vortex sheet has not become completely rolled up into the vortex core. On the wing used in the present investigation, apparently only a comparatively small amount of vorticity exists outside the region of the vortex core.

#### Location of Vortex Cores

The vertical locations of the vortex cores have been obtained from the photographs of figure 5 and are plotted in figure 7. In general,

the vortex cores appear to leave the wing at approximately the 12.5-percent-chord position with an initial slope somewhat less than the angle of attack of the wing. The slopes of the vortex cores are approximately equal to one-half the angle of attack at the trailing edge of the wing and decrease somewhat behind the trailing edge. For the purposes of comparison, the theoretical slopes of the free vortices for a rectangular wing of aspect ratio 0.25 have been calculated according to the theory of reference 4 and are plotted in figure 7 as springing from the quarter-chord position. The theoretical slopes approximate the experimental slopes very well, being only slightly greater than the experimental slopes at small angles of attack and slightly less than the experimental slopes at large angles of attack.

The lateral movement of the vortex cores with angle of attack appears to be negligible, although the exact lateral location of the cores is difficult to estimate from the photographs. In general, the photographs show no clearly defined inward movement as would be expected on wings of higher aspect ratio or on delta and swept wings.

#### Chordwise Growth of Lift

On the basis that the tuft projections in the vertical and horizontal directions are assumed to be proportional to the angles of downwash and sidewash, it is possible to calculate the circulation around a vortex at the chordwise locations considered. A square of convenient size enclosing the vortex at a particular chord position was chosen and the tuft projections on the perimeter of the square were estimated and plotted as shown in figure 8. It was found convenient to use the photograph negatives and a low-power magnifying glass for this purpose. Inasmuch as the free-stream velocity and the total length of the tufts (3 inches) were known, the tangential velocities at the tuft locations on the perimeter of the square could be obtained. The tangential velocity at each tuft location was used as the average tangential velocity for a 1-inch path and integration around the closed-square path gave the circulation of the vortex:

$$\Gamma = \oint V_t \, ds$$

where

$$V_t = \frac{\text{Tuft projection}}{\text{Length of tuft}} \times V$$

The circulation of the vortices was calculated for all grid positions for several angles of attack. The average circulation of the right and left vortices was used with the assumption of a simple horse-

shoe vortex pattern in order to interpret the results in terms of the lift coefficient at the various grid positions. Each calculation was performed twice independently.

The results of calculations for angles of attack of  $10^\circ$ ,  $14^\circ$ ,  $20^\circ$ , and  $24^\circ$  are presented in figure 9 as total lift coefficient at each chord position plotted against grid position. The lift increases fairly rapidly across the forward part of the chord with approximately 70 to 85 percent of the total wing lift present forward of the midchord position, depending on the angle of attack. The growth of lift, in all cases, approaches asymptotically the value of the lift measured in the force tests and the agreement is very good. The fact that the calculated lift is in close agreement with the measured lift is a good indication that most or all of the vorticity is concentrated in the two rolled-up vortices.

A comparison of the values calculated from tuft photographs with the theoretical chordwise loading results of reference 6 is shown in figure 10 as a function of the ratio of the total lift coefficient at the specified chord position to the total lift coefficient of the wing. The theoretical chordwise loading of reference 6 indicates a center-of-pressure position much nearer the leading edge than that of the experimental results for  $\alpha$  from  $10^\circ$  to  $24^\circ$ . This effect is verified qualitatively by the center-of-pressure positions shown in figure 3(b). The results, calculated from the photographs and presented in figure 10, indicate that the smallest angle of attack considered ( $\alpha = 10^\circ$ ) gives the best results, as would be expected; however, the results are similar for all angles of attack considered and the results for  $\alpha = 24^\circ$  are in closer agreement than those for  $\alpha = 20^\circ$ .

### CONCLUSIONS

Studies of the flow characteristics in the vicinity of a modified flat-plate rectangular wing of aspect ratio 0.25 made by the use of photographs of a tuft grid located at various chordwise positions and supplemented by tests with a yaw-head pitot-tube installation have resulted in the following conclusions:

1. There is a rapid rolling-up of the trailing vorticity along the chord of the wing and, at the higher angles of attack, a distinct vortex is visible at the first chordwise station behind the leading edge considered (12.5 percent chord). The trailing vortex sheet is apparently immediately rolled up into the vortex cores.
2. The vertical locations of the vortex cores appear to leave the wing at approximately the 12.5-percent-chord position with an initial

slope somewhat less than the angle of attack of the wing. The slope is approximately equal to one-half the angle of attack of the wing at the trailing edge and decreases somewhat behind the trailing edge. The slopes of the vertical locations of the vortex cores are predicted very well by the theory of Bollay. The photographs show no clearly defined lateral movement of the cores with increasing angle of attack.

3. The chordwise growth of lift calculated from the vortex circulation shows that the lift increases fairly rapidly across the forward part of the chord, with approximately 70 to 85 percent of the total wing lift present forward of the midchord position. The total lift calculated from the tuft-grid photographs showed good agreement with the lift measured on the balance system.

Langley Aeronautical Laboratory,  
National Advisory Committee for Aeronautics,  
Langley Field, Va., June 11, 1952.

#### REFERENCES

1. Voepel, H.: Tests on Wings of Small Aspect Ratio. Library Translation No. 276, British R.A.E., Oct. 1948.
2. Bird, John D., and Riley, Donald R.: Some Experiments on Visualization of Flow Fields Behind Low-Aspect-Ratio Wings by Means of a Tuft Grid. NACA TN 2674, 1952.
3. Winter, H.: Flow Phenomena on Plates and Airfoils of Short Span. NACA TM 798, 1936.
4. Bollay, William: A Non-Linear Wing Theory and Its Application to Rectangular Wings of Small Aspect Ratio. Z.f.a.M.M., Bd. 19, Nr. 1, Feb. 1939, pp. 21-35.
5. Weinig, F.: Lift and Drag of Wings With Small Span. NACA TM 1151, 1947.
6. Wieghardt, Karl: Chordwise Load Distribution of a Simple Rectangular Wing. NACA TM 963, 1940.
7. Allen, H. Julian: Pressure Distribution and Some Effects of Viscosity on Slender Inclined Bodies of Revolution. NACA TN 2044, 1950.
8. Spreiter, John R., and Sacks, Alvin H.: The Rolling Up of the Trailing Vortex Sheet and Its Effect on the Downwash Behind Wings. Jour. Aero. Sci., vol. 18, no. 1, Jan. 1951, pp. 21-32, 72.

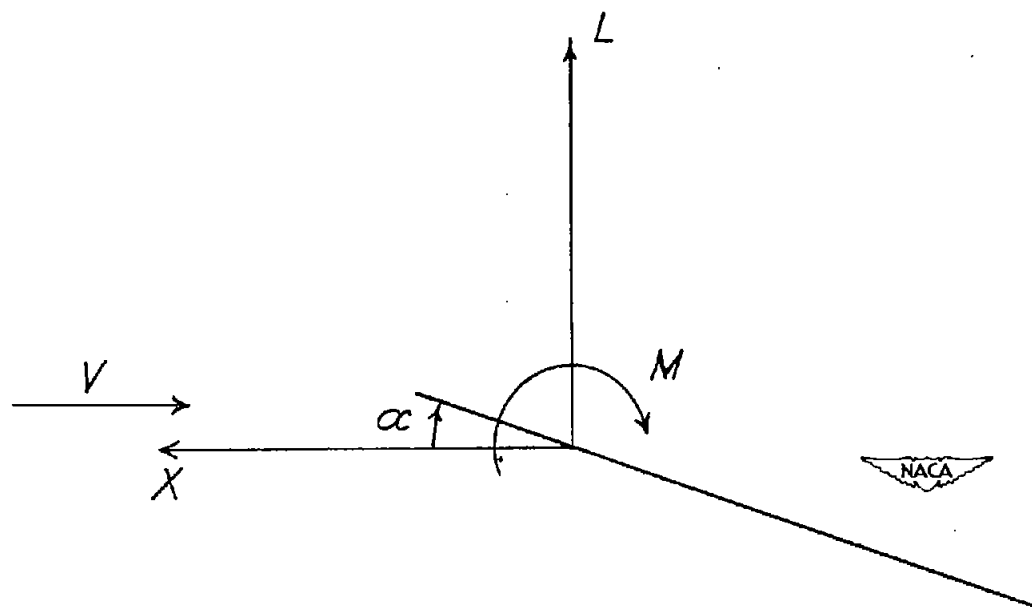
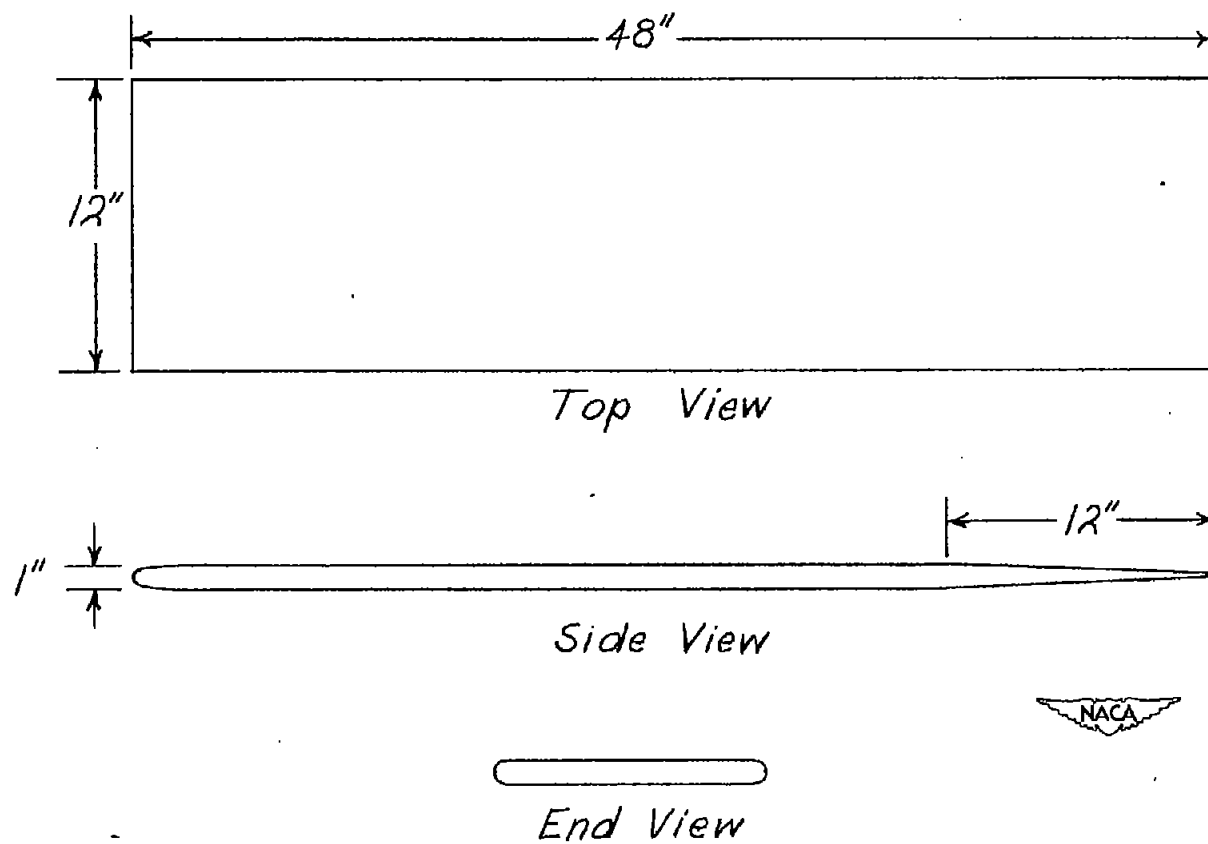
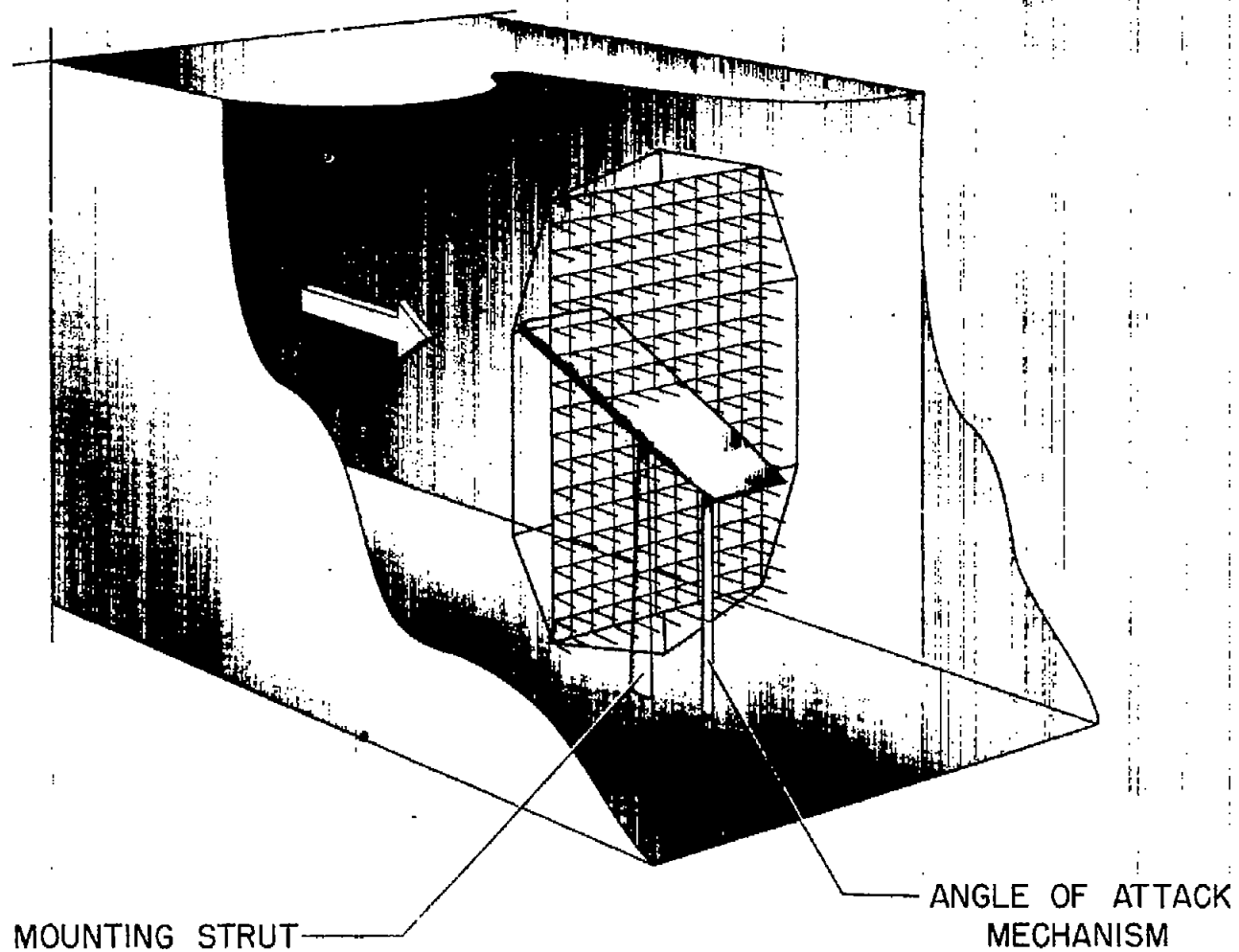


Figure 1.- System of axes used. Arrows indicate positive directions of forces, moment, and angle.



(a) Views of model.

Figure 2.- Views of model used in this investigation and tunnel setup.

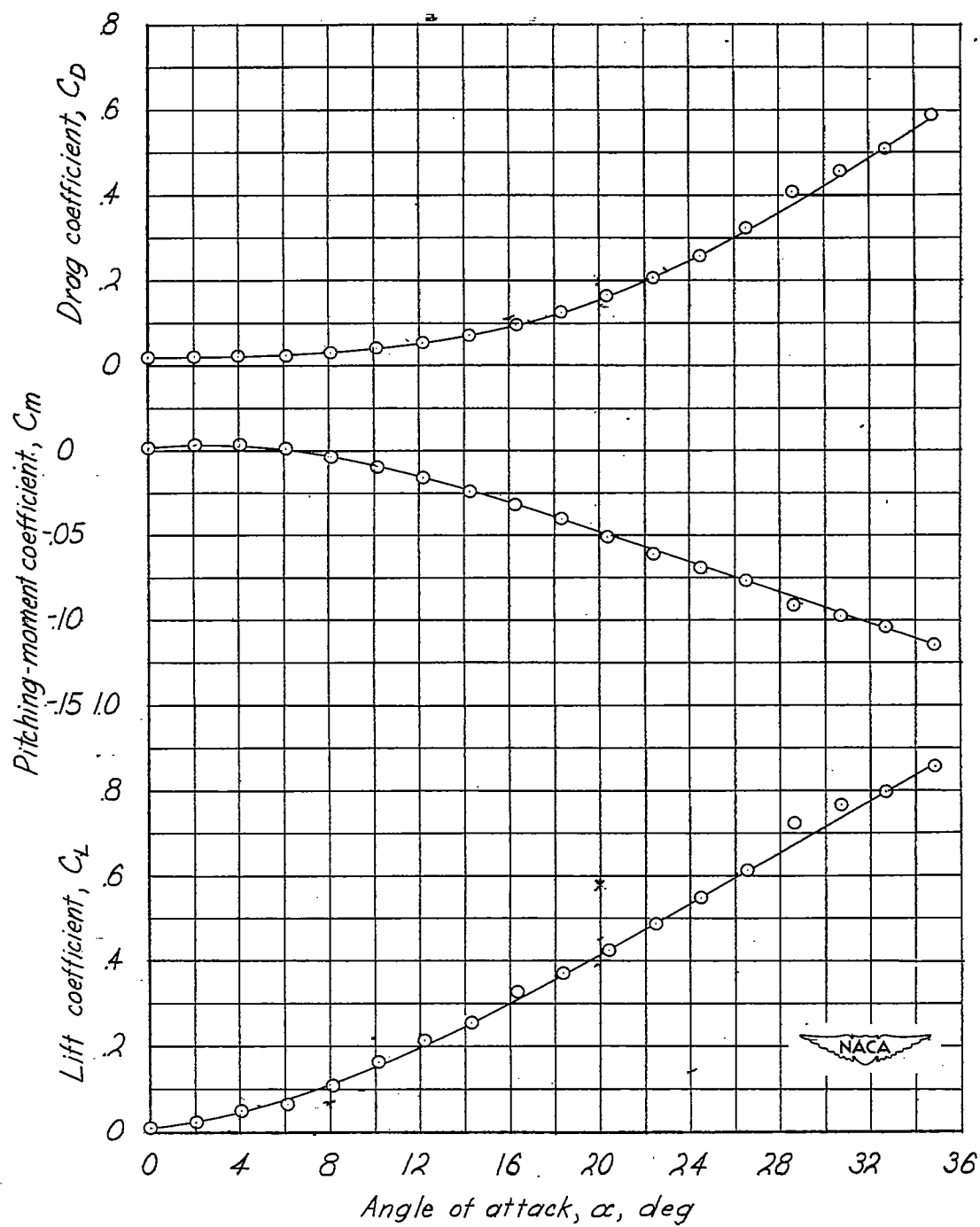


(b) Cutaway drawing of tunnel setup.

Figure 2.- Concluded.

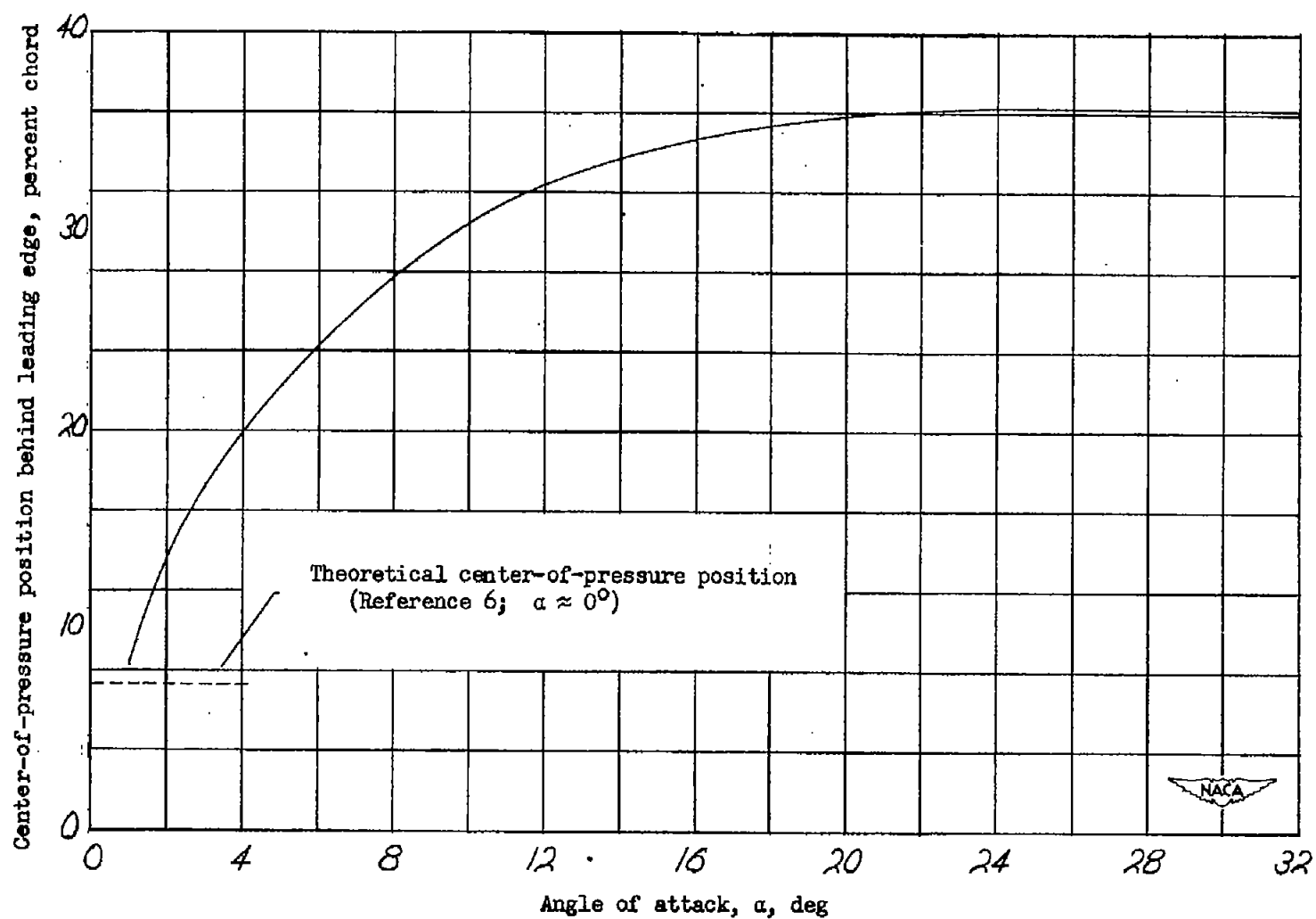


L-75154



(a) Lift, pitching-moment, and drag coefficients.

Figure 3.- Aerodynamic characteristics of wing of aspect ratio 0.25.  
Reynolds number,  $2.09 \times 10^6$ .



(b) Position of center of pressure.

Figure 3.- Concluded.

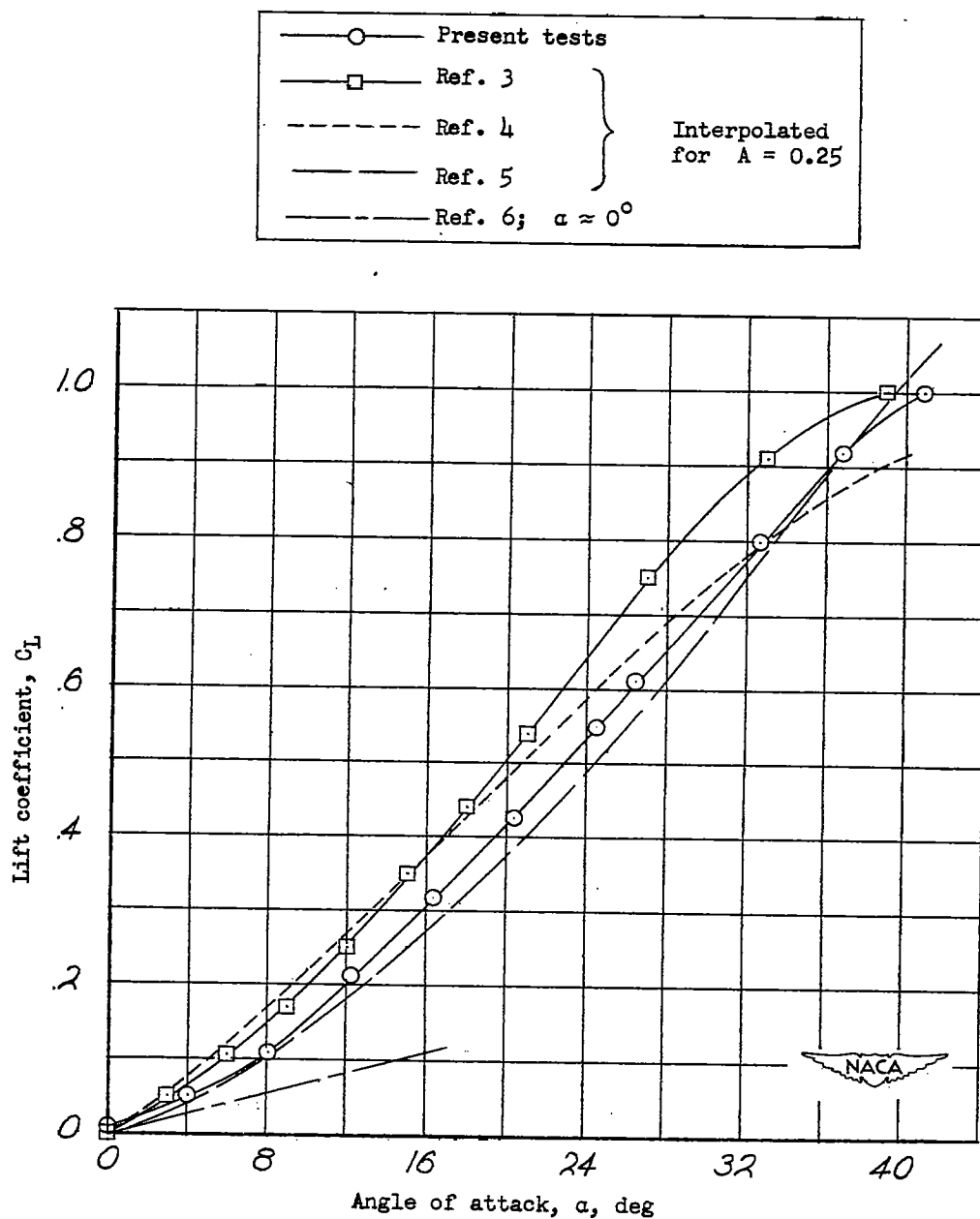
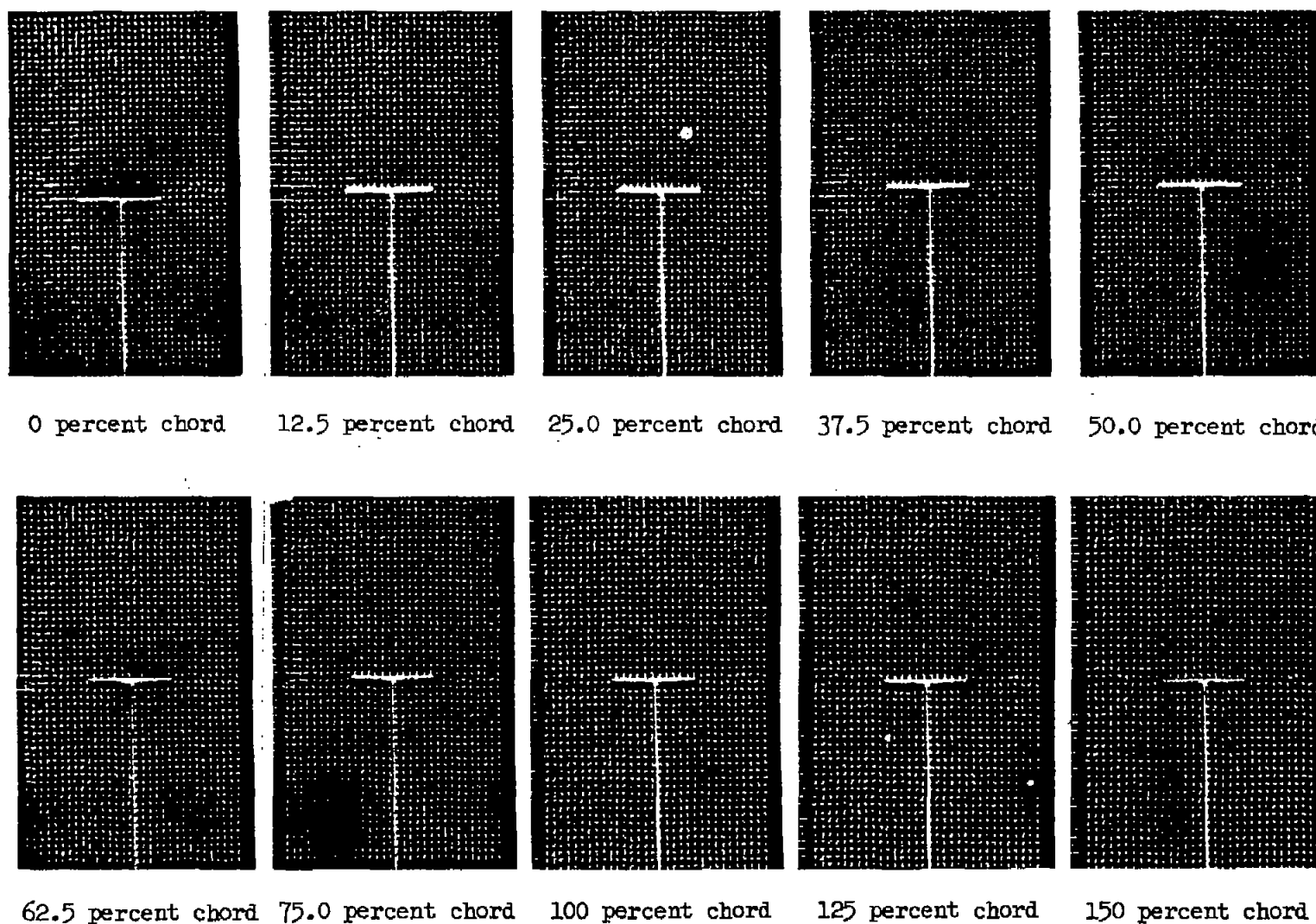


Figure 4.- Comparison of lift curves of a rectangular wing of aspect ratio 0.25 obtained from various sources.

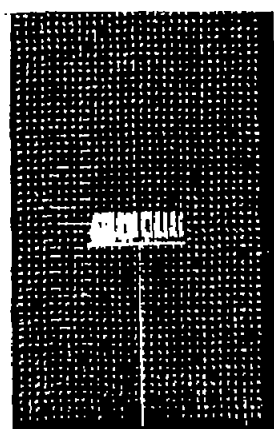


(a)  $\alpha = 0^\circ$ .

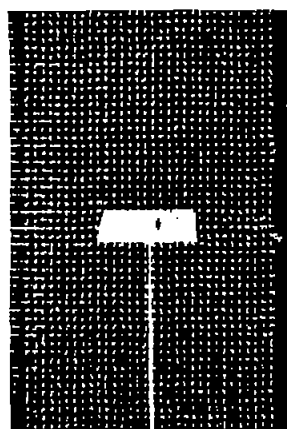


L-75155

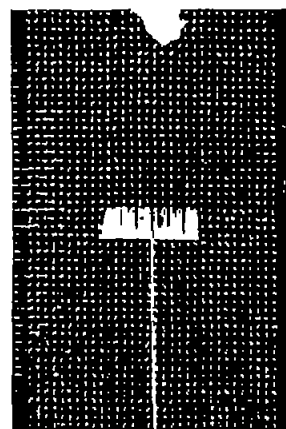
Figure 5.- Tuft grid located at various chordwise positions on a modified flat-plate rectangular wing of aspect ratio 0.25.



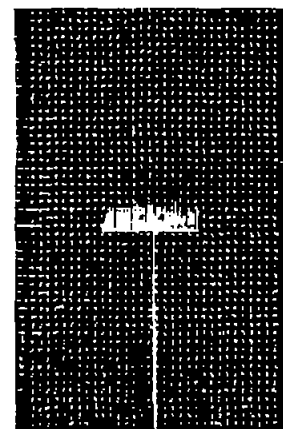
0 percent chord



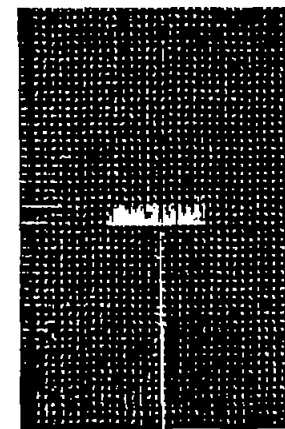
12.5 percent chord



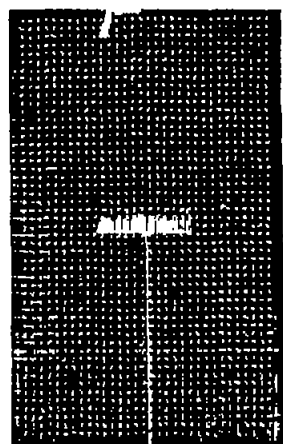
25.0 percent chord



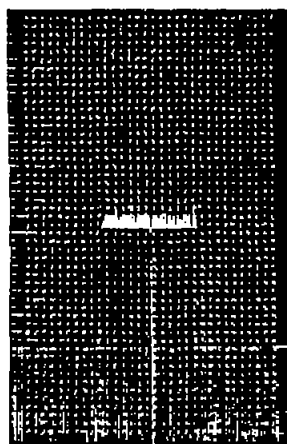
37.5 percent chord



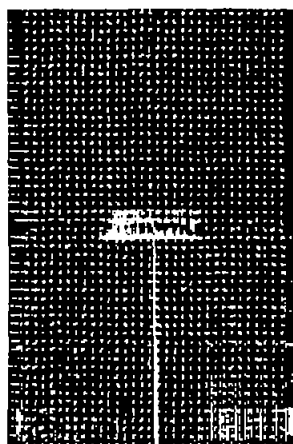
50.0 percent chord



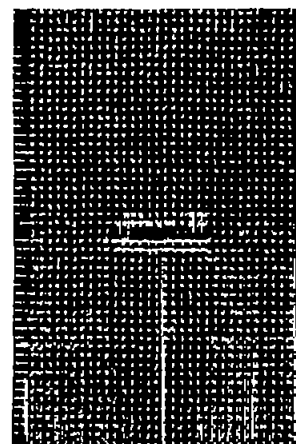
62.5 percent chord



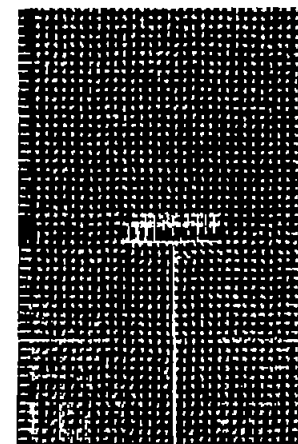
75.0 percent chord



100 percent chord



125 percent chord



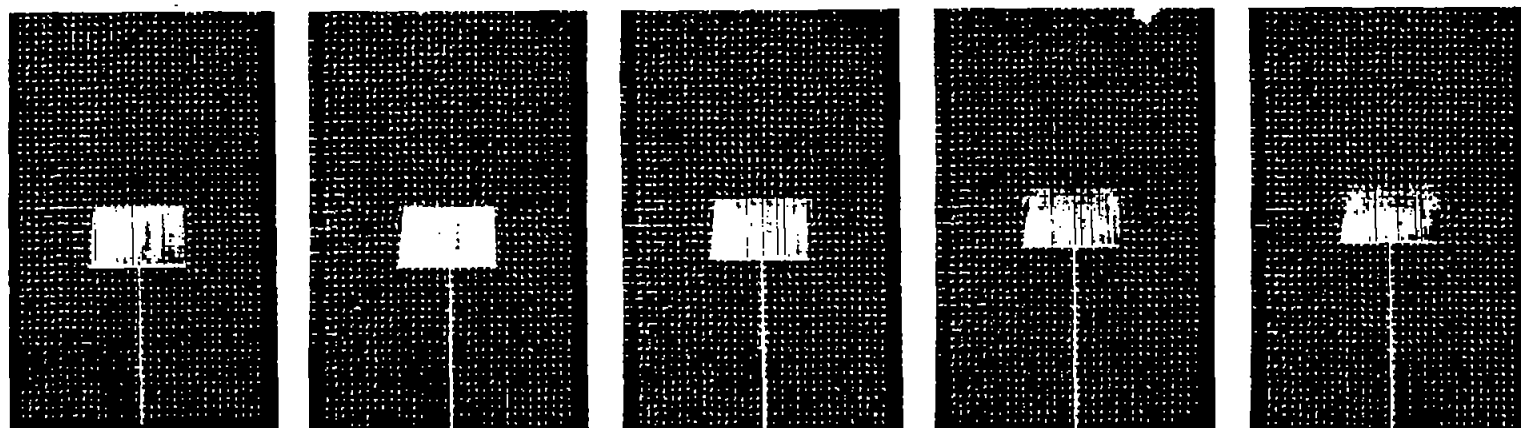
150 percent chord

(b)  $\alpha = 4^\circ$ .

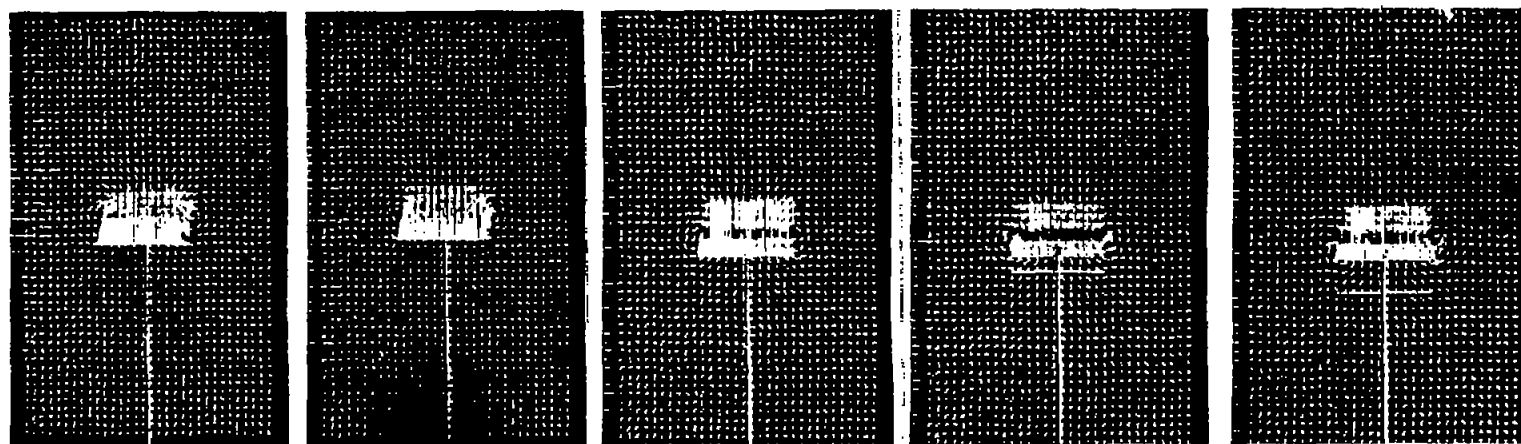
Figure 5.- Continued.



L-75156



0 percent chord    12.5 percent chord    25.0 percent chord    37.5 percent chord    50.0 percent chord



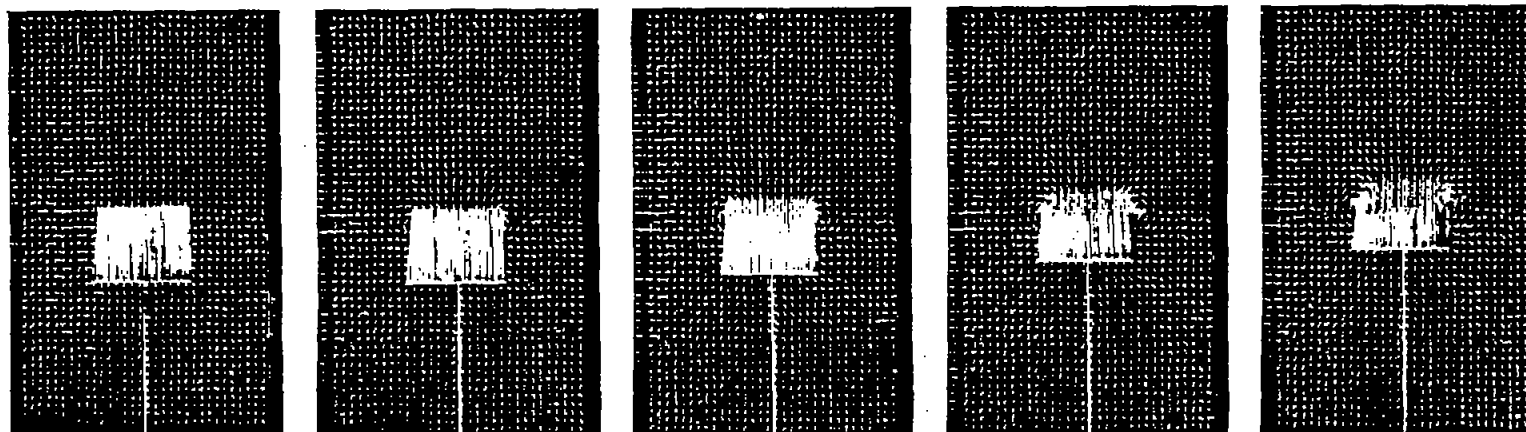
62.5 percent chord    75.0 percent chord    100 percent chord    125 percent chord    150 percent chord

(c)  $\alpha = 8^\circ$ .

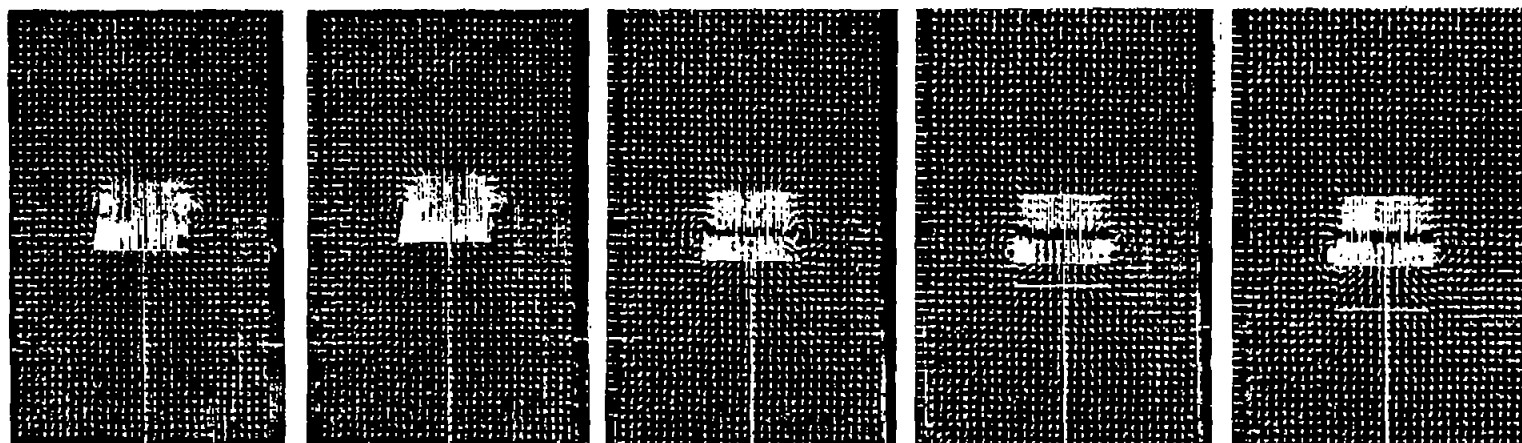
Figure 5.- Continued.



L-75157



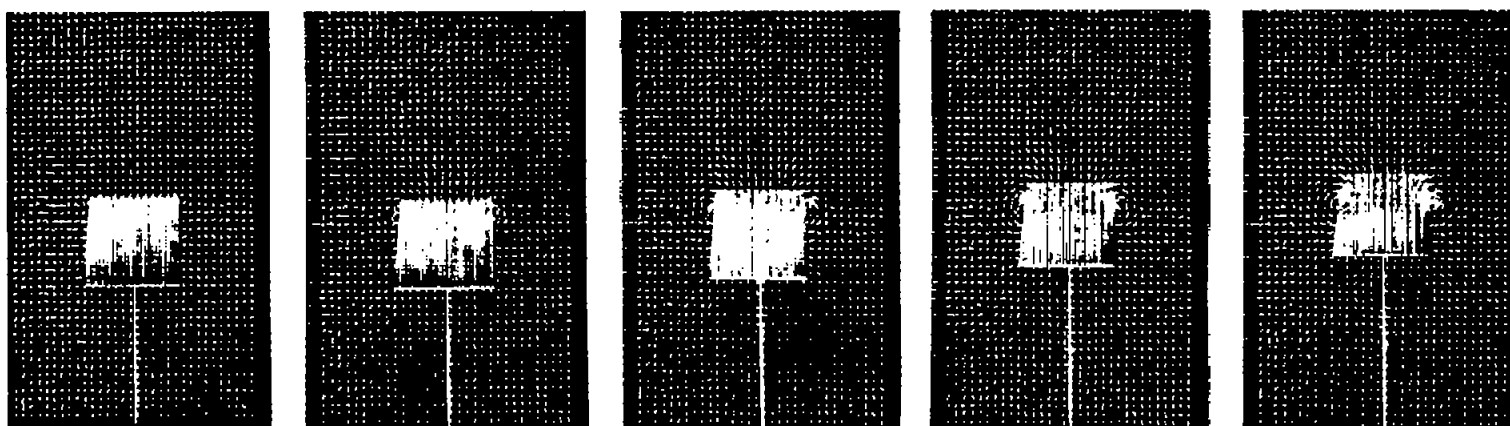
0 percent chord    12.5 percent chord    25.0 percent chord    37.5 percent chord    50.0 percent chord



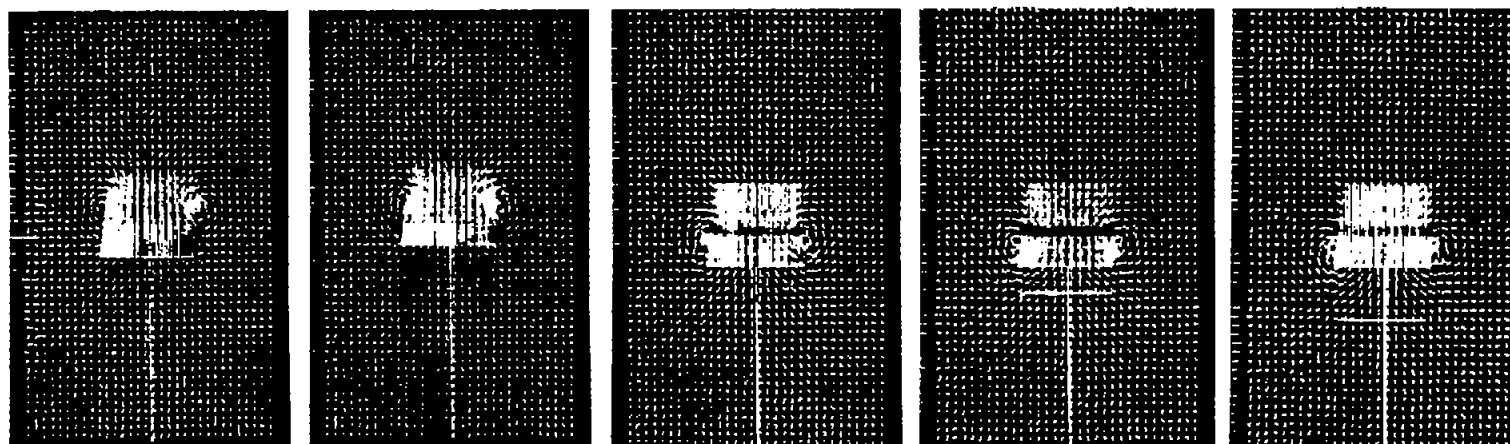
62.5 percent chord    75.0 percent chord    100 percent chord    125 percent chord    150 percent chord

(d)  $\alpha = 10^\circ$ .

Figure 5.- Continued.



0 percent chord    12.5 percent chord    25.0 percent chord    37.5 percent chord    50.0 percent chord

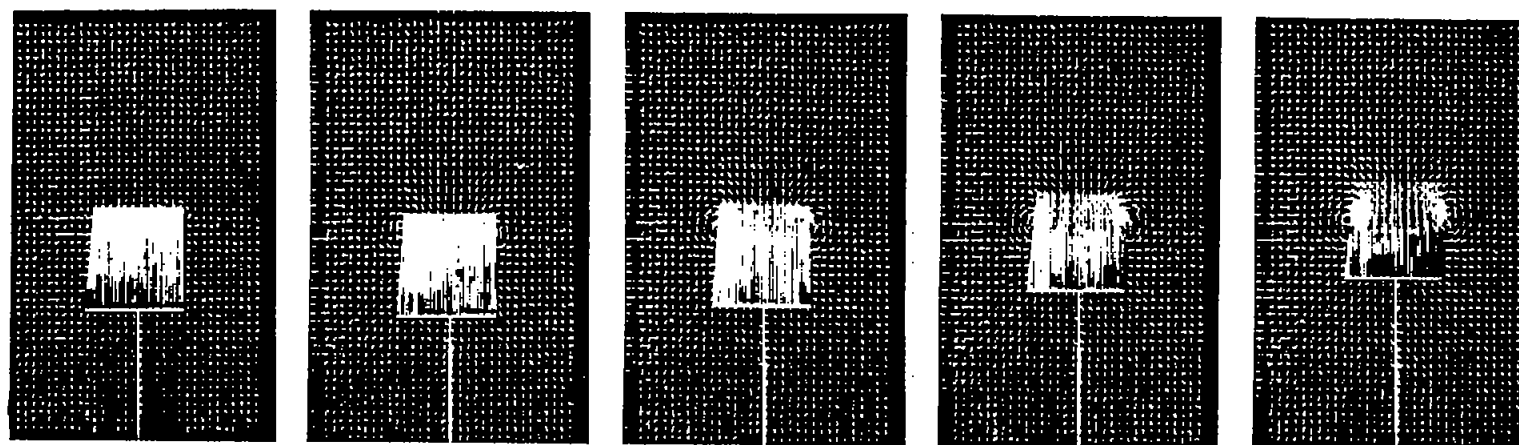


62.5 percent chord    75.0 percent chord    100 percent chord    125 percent chord    150 percent chord

(e)  $\alpha = 12^\circ$ .

Figure 5.- Continued.

NACA  
L-75159



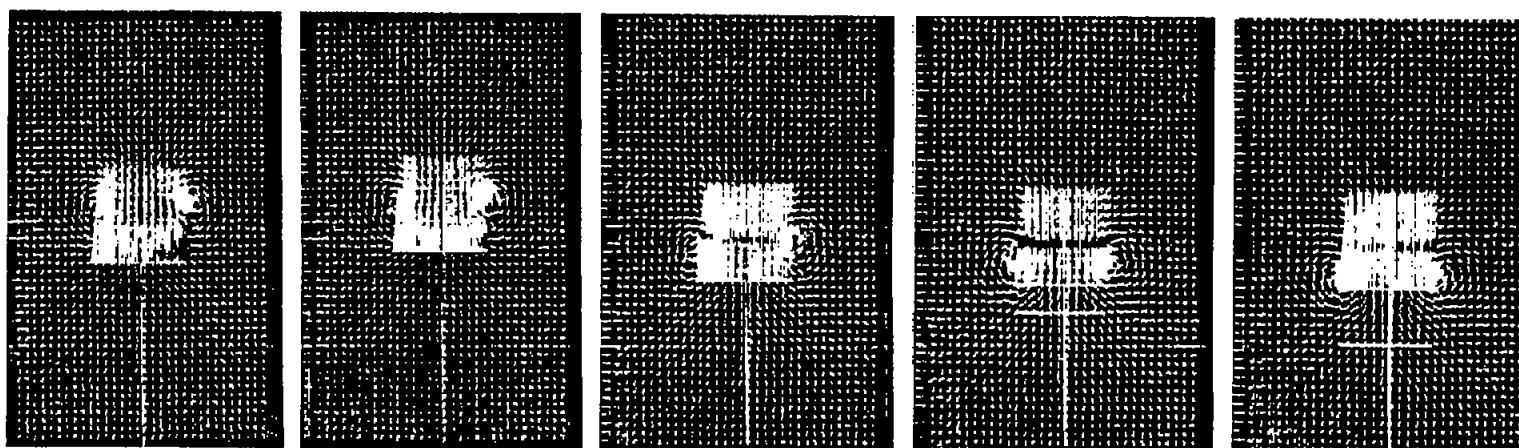
0 percent chord

12.5 percent chord

25.0 percent chord

37.5 percent chord

50.0 percent chord



62.5 percent chord

75.0 percent chord

100 percent chord

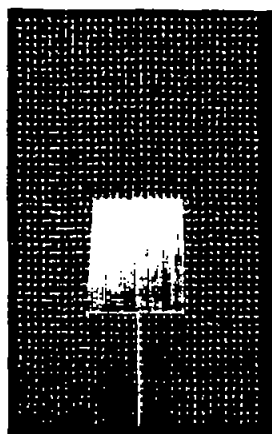
125 percent chord

150 percent chord

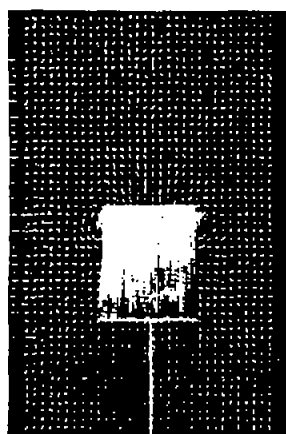
(f)  $\alpha = 14^\circ$ .

Figure 5.- Continued.

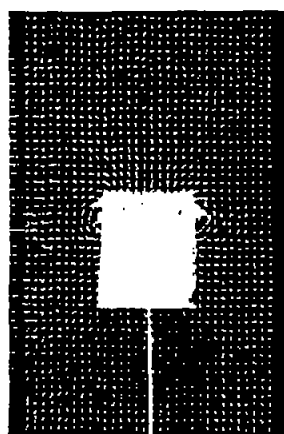
NACA  
L-75160



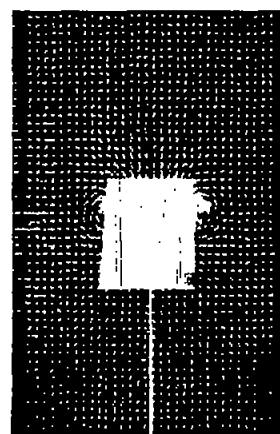
0 percent chord



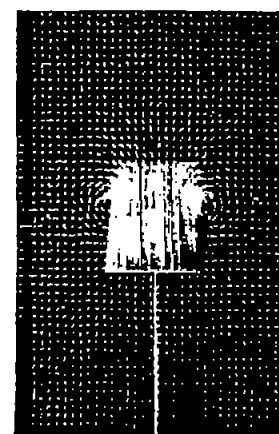
12.5 percent chord



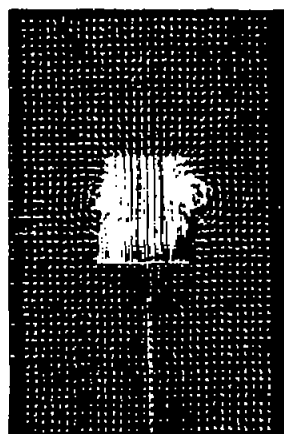
25.0 percent chord



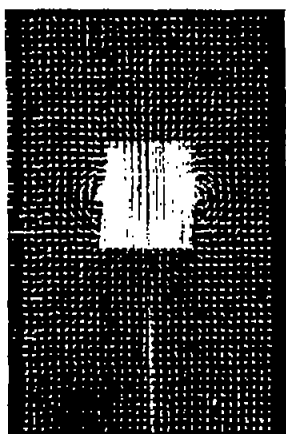
37.5 percent chord



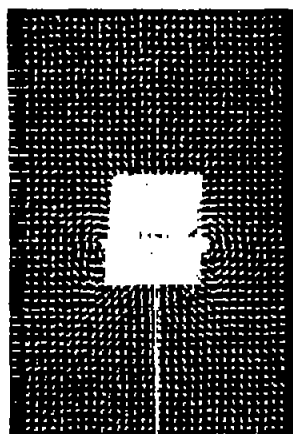
50.0 percent chord



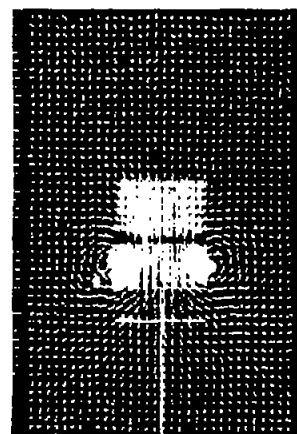
62.5 percent chord



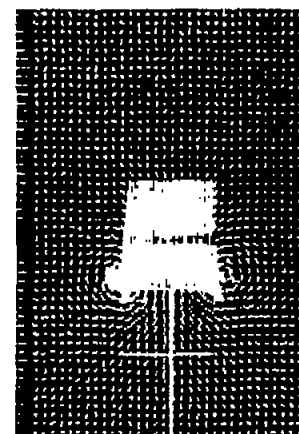
75.0 percent chord



100 percent chord



125 percent chord

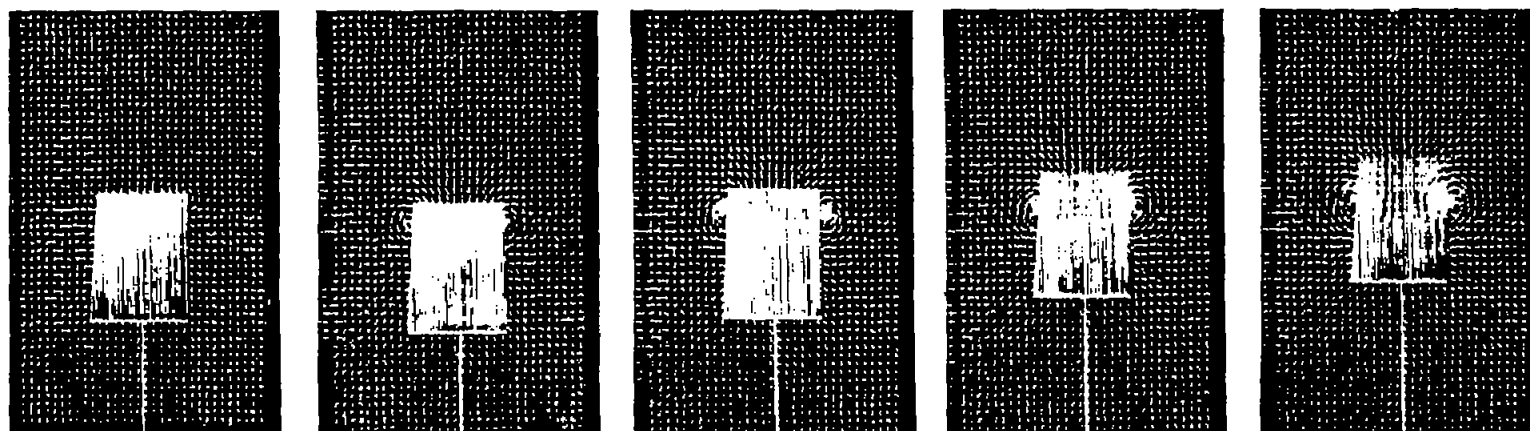


150 percent chord

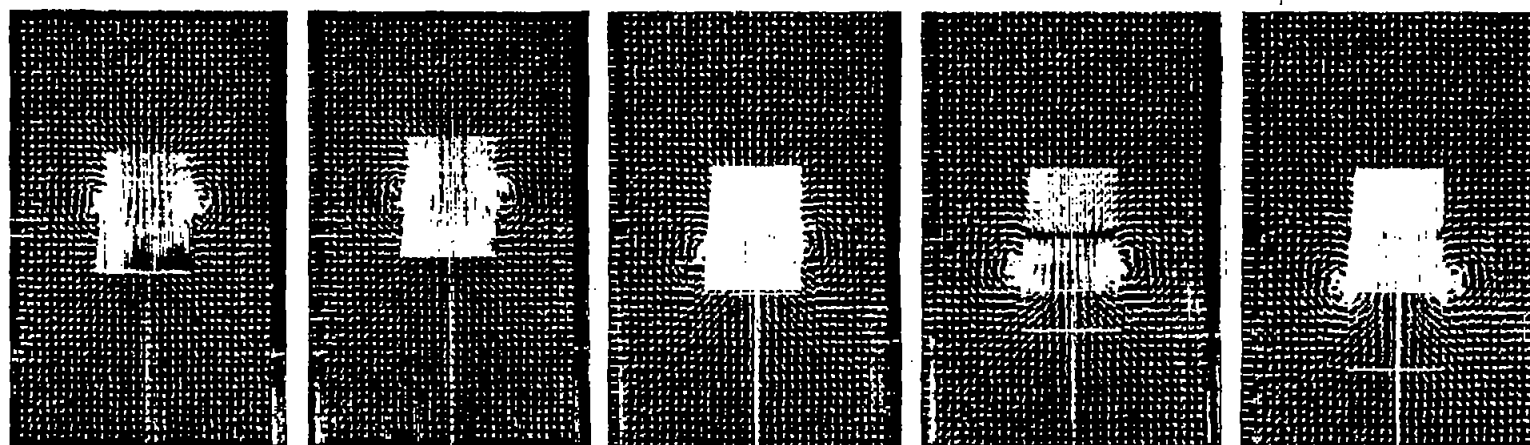
(g)  $\alpha = 16^\circ$ .

Figure 5.- Continued.

NACA  
L-75161



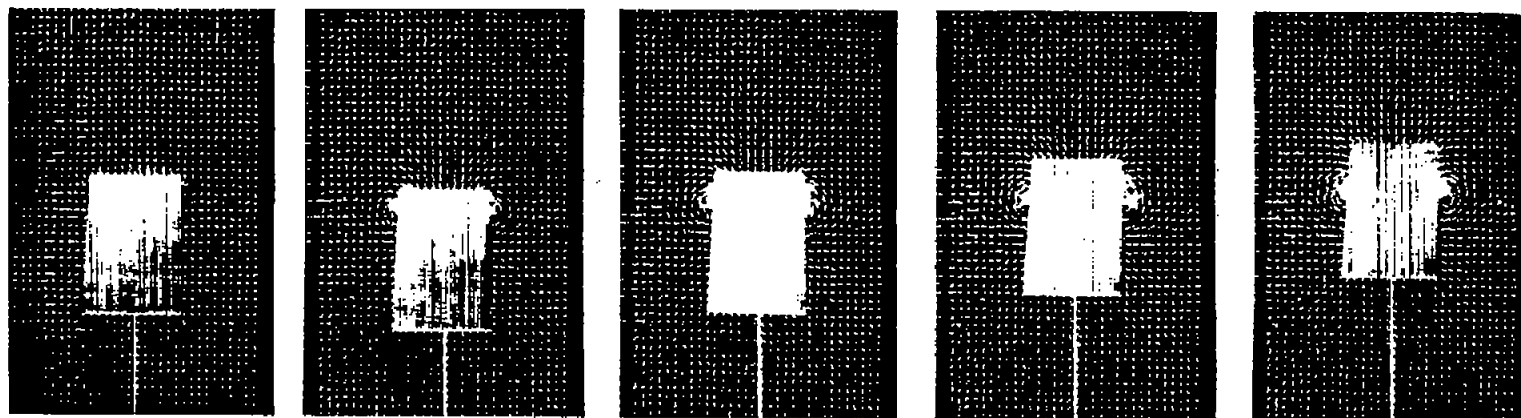
0 percent chord    12.5 percent chord    25.0 percent chord    37.5 percent chord    50.0 percent chord



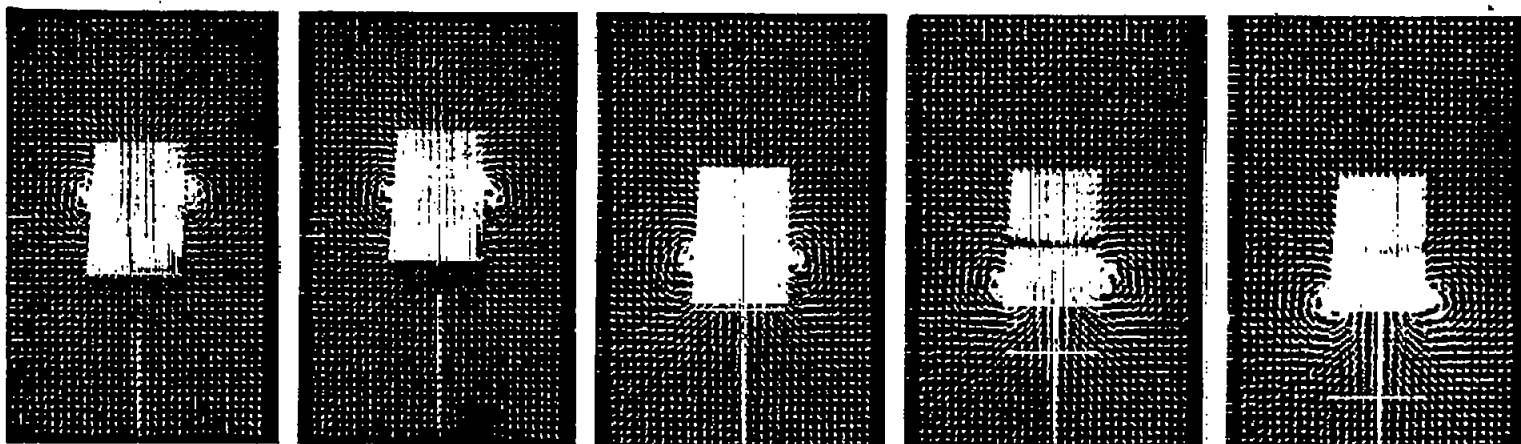
62.5 percent chord    75.0 percent chord    100 percent chord    125 percent chord    150 percent chord

(h)  $\alpha = 18^\circ$ .

Figure 5.- Continued.



0 percent chord    12.5 percent chord    25.0 percent chord    37.5 percent chord    50.0 percent chord

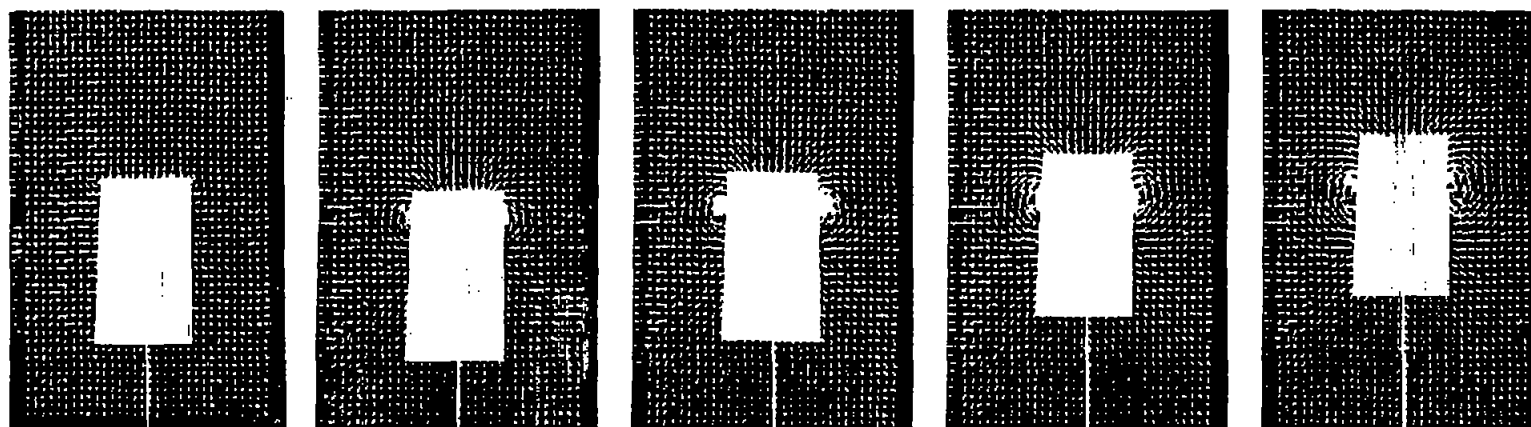


62.5 percent chord    75.0 percent chord    100 percent chord    125 percent chord    150 percent chord

(i)  $\alpha = 20^\circ$ .

Figure 5.- Continued.

NACA  
L-75163



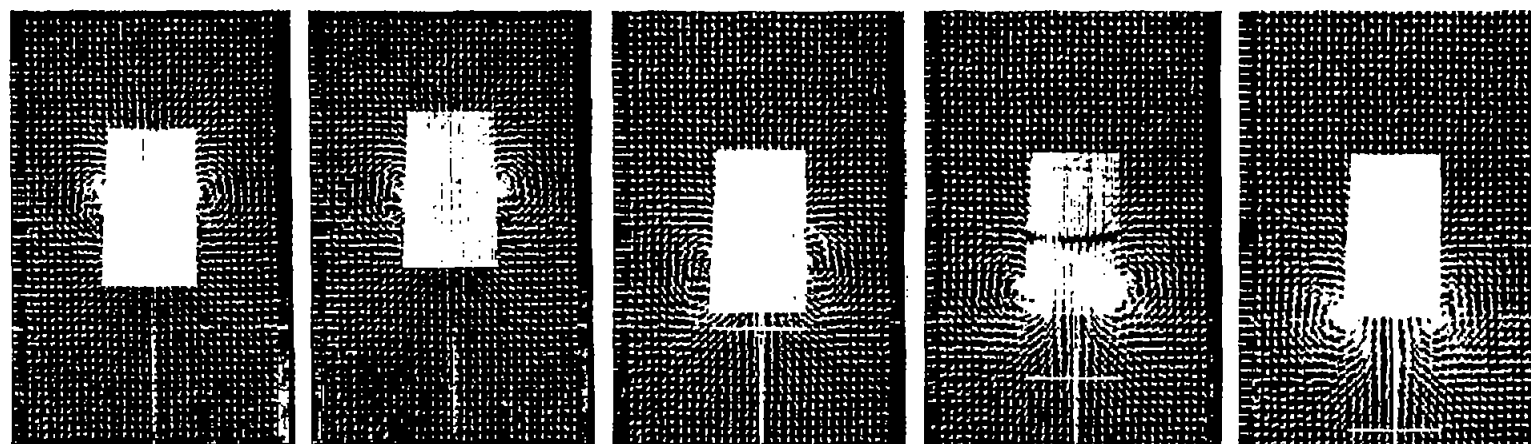
0 percent chord

12.5 percent chord

25.0 percent chord

37.5 percent chord

50.0 percent chord



62.5 percent chord

75.0 percent chord


100 percent chord

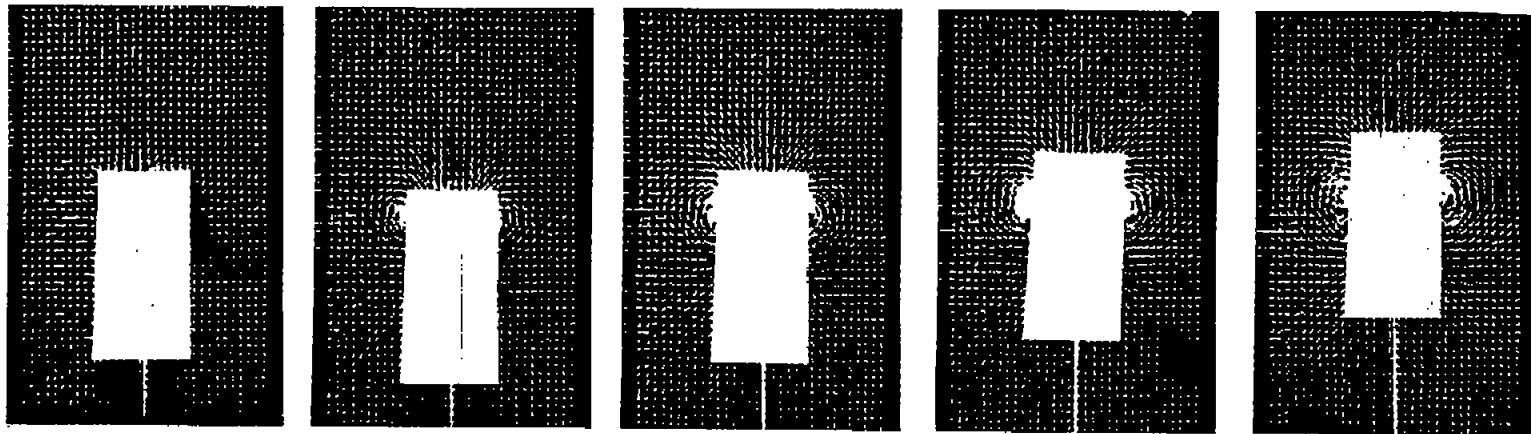
125 percent chord

150 percent chord

(j)  $\alpha = 24^\circ$ .

Figure 5.- Continued.

  
 L-75164



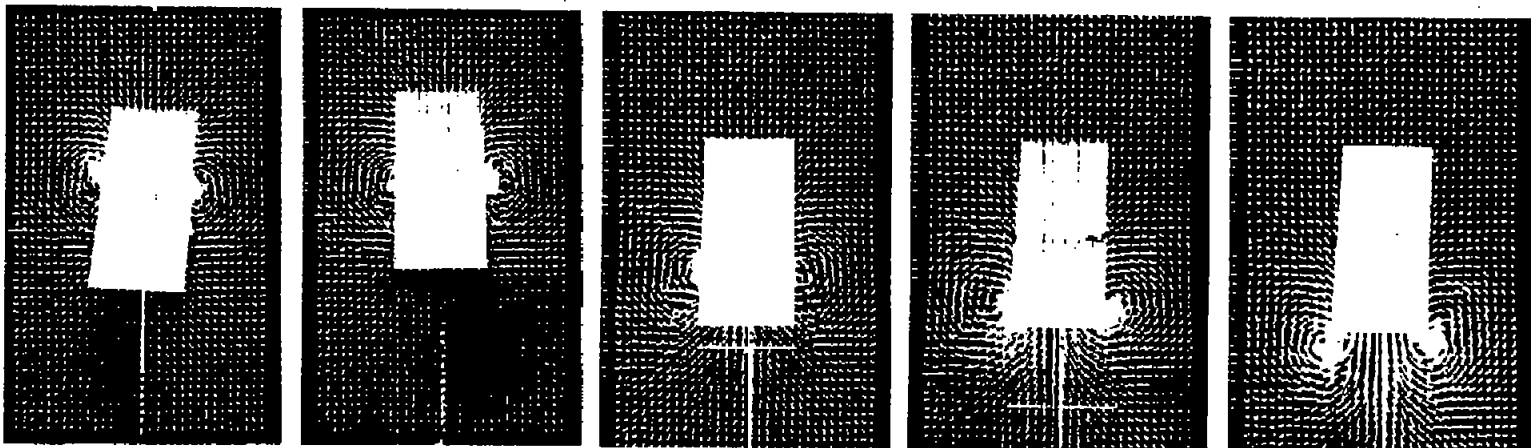
0 percent chord

12.5 percent chord

25.0 percent chord

37.5 percent chord

50.0 percent chord



62.5 percent chord

75.0 percent chord


100 percent chord

125 percent chord

150 percent chord

(k)  $\alpha = 28^\circ$ .

Figure 5.- Concluded.


 NACA  
L-75165

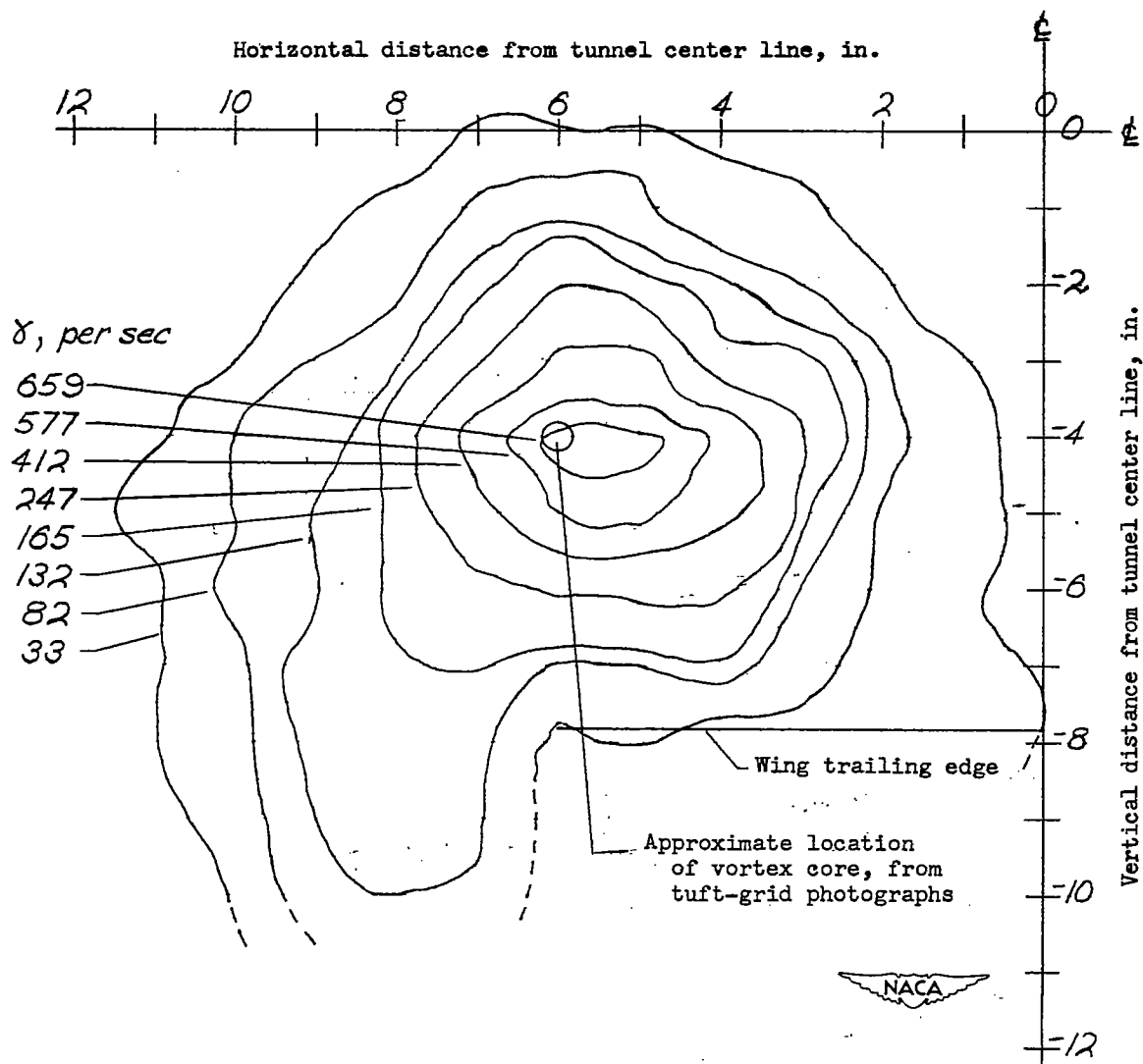


Figure 6.- Vorticity distribution in plane approximately 3.5 inches (7 percent chord) behind trailing edge of a modified flat-plate rectangular wing of aspect ratio 0.25. Contours are of equal vorticity. Angle of attack,  $20^\circ$ ; Reynolds number,  $2.09 \times 10^6$ .

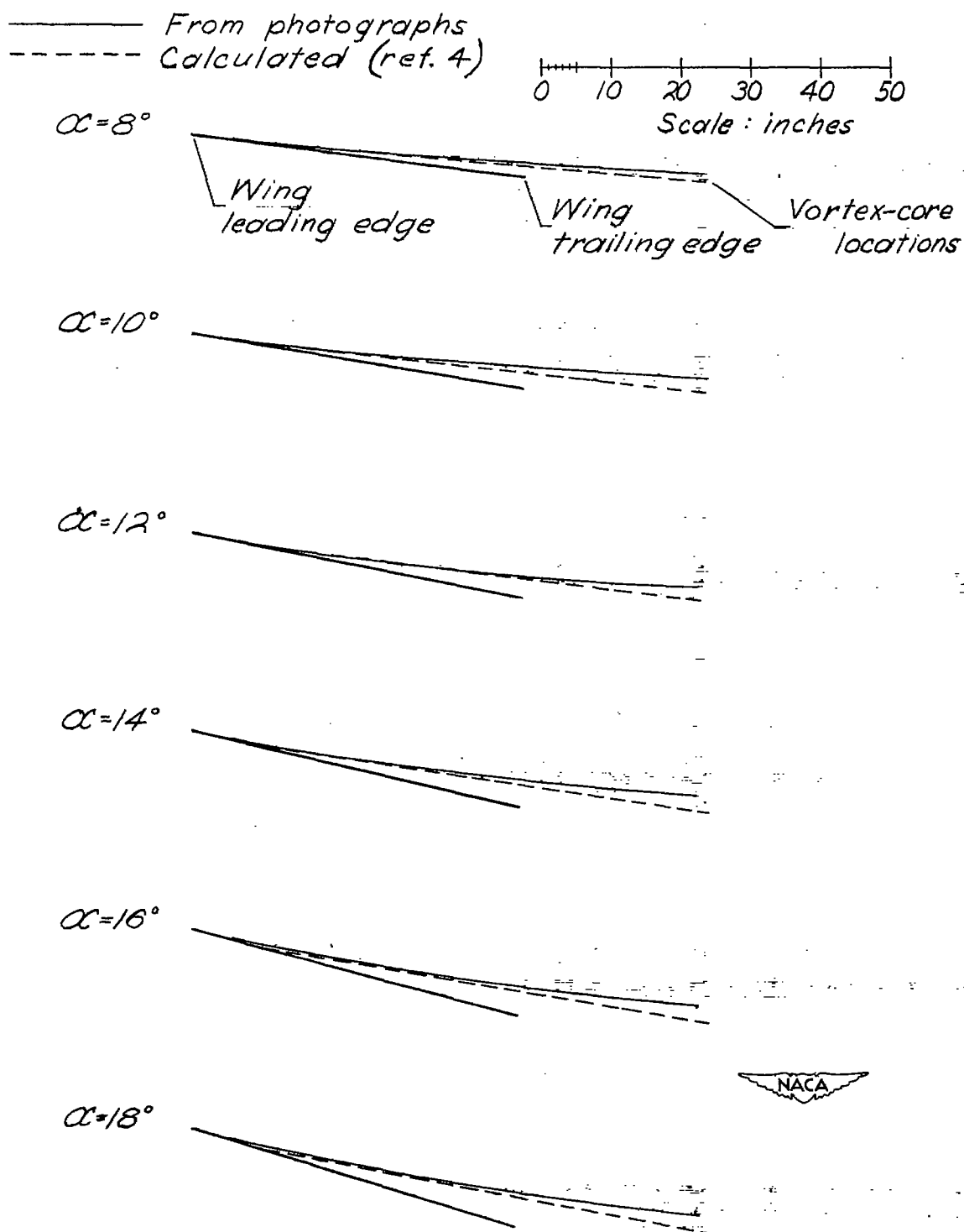
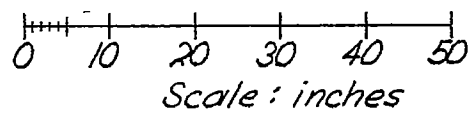


Figure 7.- Vortex-core locations in the vertical plane for a modified flat-plate rectangular wing of aspect ratio 0.25.

———— From photographs  
----- Calculated (ref. 4)



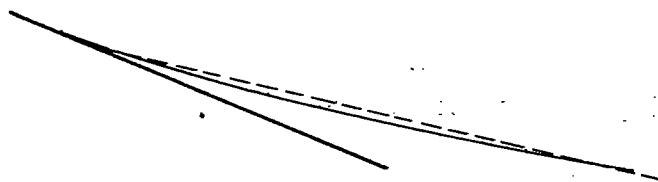
$\alpha = 20^\circ$



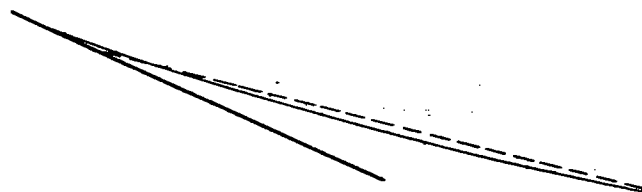
$\alpha = 22^\circ$



$\alpha = 24^\circ$



$\alpha = 26^\circ$



$\alpha = 28^\circ$

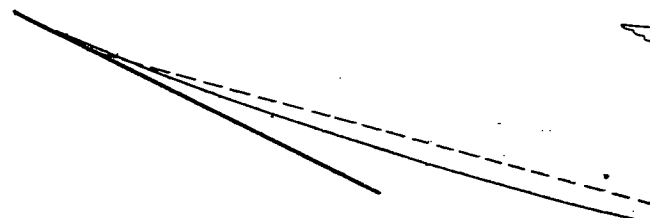
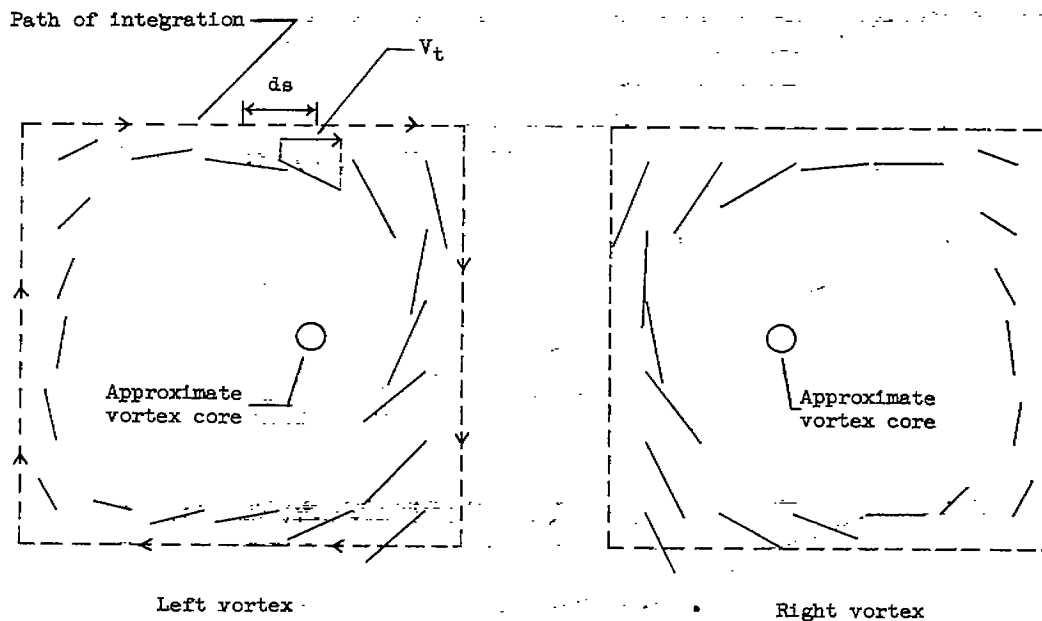


Figure 7.- Concluded.



$$V_t = \frac{\text{Tuft projection}}{\text{Length of tuft}} \times V$$

$$\Gamma = \oint V_t ds$$

$$C_{L\text{chord}} = \frac{2\Gamma}{cV}$$



Figure 8.- Calculation of the circulation in the wing wake from photographs of a tuft grid. Grid at trailing edge.  $\alpha = 140^\circ$ .

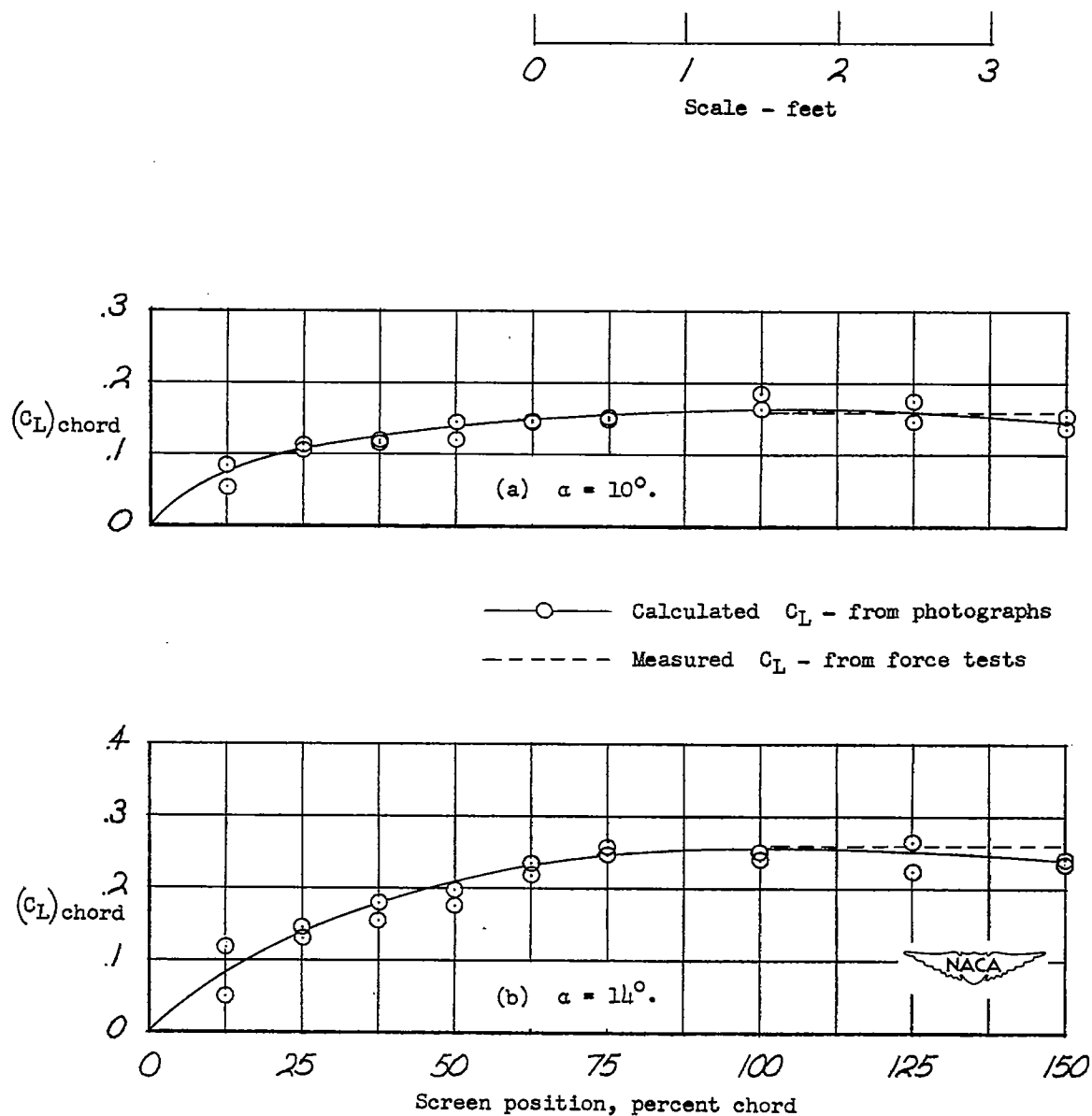
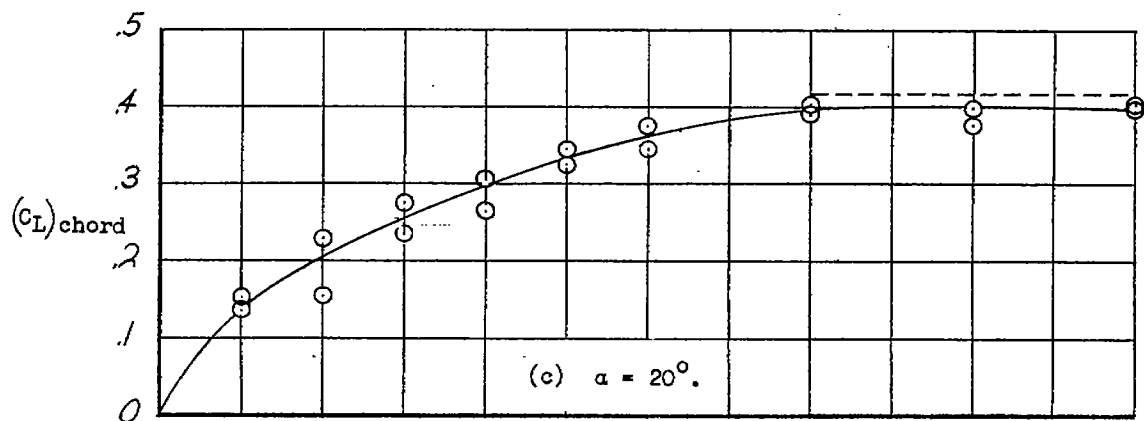


Figure 9.- Chordwise growth of lift on modified flat-plate wing of aspect ratio 0.25 for several angles of attack. Calculated from trailing-vortex strengths using tuft-grid photographs. Wing chord, 48 inches.



—○— Calculated  $C_L$  - from photographs

----- Measured  $C_L$  - from force tests

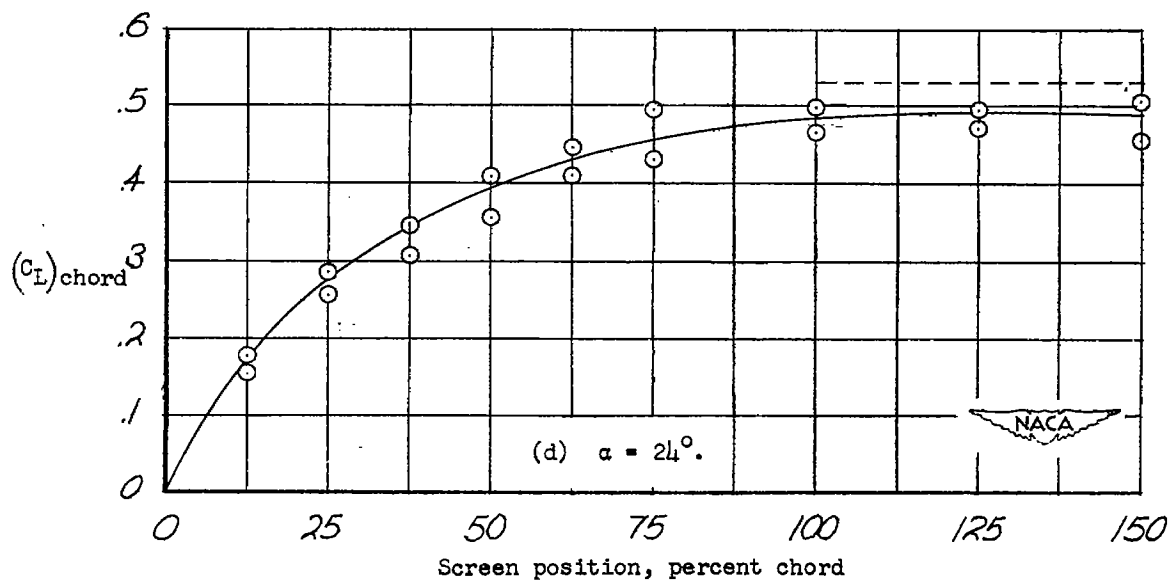


Figure 9.- Concluded.

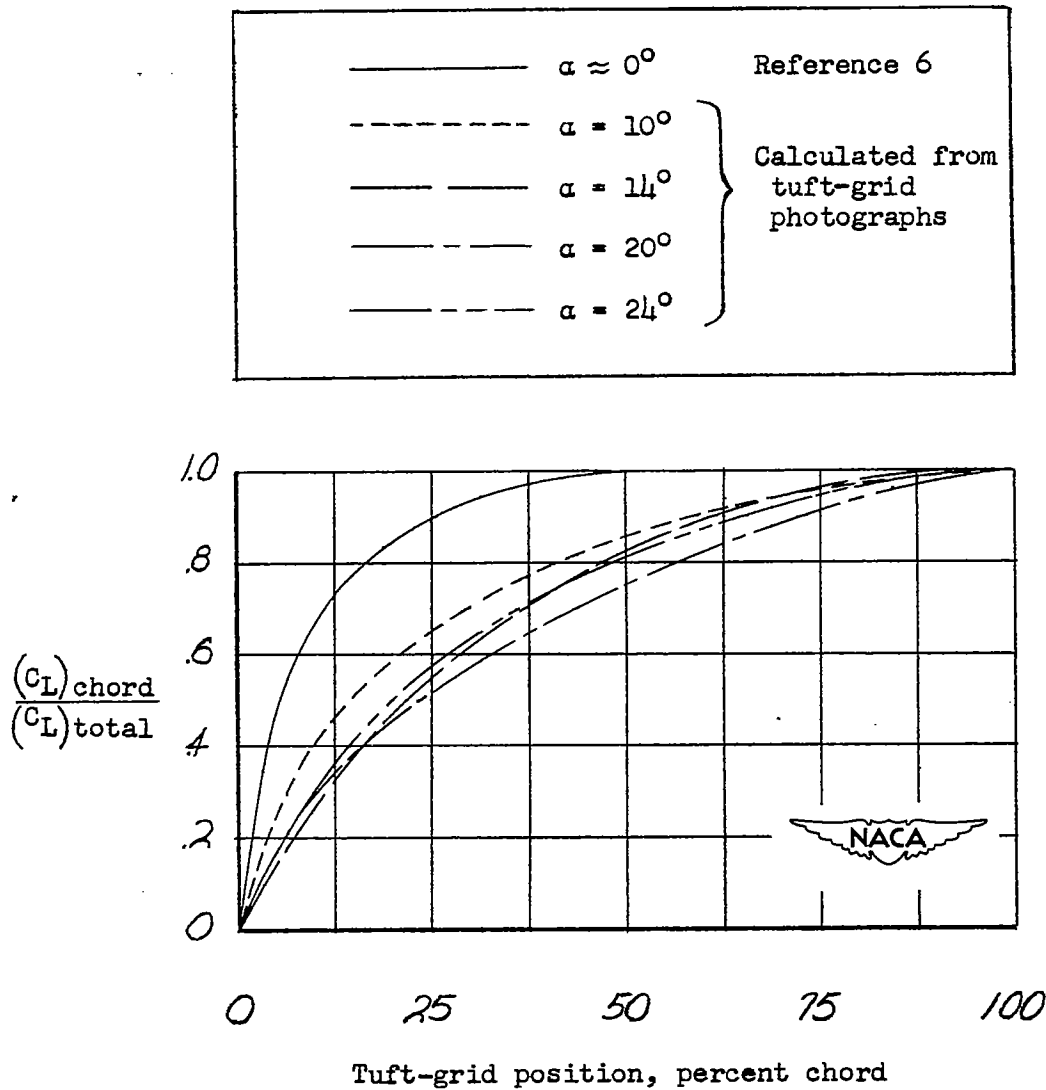


Figure 10.- Chordwise growth of lift on modified flat-plate wing of aspect ratio 0.25. Comparison of theoretical values and values calculated from tuft-grid photographs. Wing chord, 48 inches.